AD-A285 868

Detection Performance of Power-Law Processors for Random Signals of Unknown Location, Structure, Extent, and Strength

Albert H. Nuttall
Surface Antisubmarine Warfare Directorate

94-33903

Naval Undersea Warfare Center Division
Newport, Rhode Island

94 11 1 078

PREFACE

The author of this report is located at the Naval Undersea Warfare Center Detachment, New London, CT 06320. The technical reviewer for this report was Stephen G. Greineder (Code 2121).

Reviewed and Approved: 16 September 1994

Donald W. Counsellor
Director, Surface Antisubmarine Warfare

REPORT DOCUMENTATION PAGE

1. AGENCY USE ONLY (Leave blank)	2. REPORT DATE	3. REPORT TYPE AND DATES COVERED
	16 September 1994	Progress

4. TITLE AND SUBTITLE	5. FUNDING NUMBERS
Detection Performance of Power-Law Processors for Random Signals of Unknown Location, Structure, Extent, and Strength	PE 0601152N

6. AUTHOR(S)

Albert H. Nuttall

7. PERFORMING ORGANIZATION NAME(S) AND ADDRESS(ES)	8. PERFORMING ORGANIZATION REPORT NUMBER
Naval Undersea Warfare Center Detachment 39 Smith Street New London, Connecticut 06320-5594	NUWC-NPT TR 10,751

9. SPONSORING/MONITORING AGENCY NAME(S) AND ADDRESS(ES)	10. SPONSORING/MONITORING AGENCY REPORT NUMBER
Office of Naval Research 800 North Quincy Street, BCT 1 Arlington, VA 22217-5000	

11. SUPPLEMENTARY NOTES

12a. DISTRIBUTION/AVAILABILITY STATEMENT	12b. DISTRIBUTION CODE
Approved for public release; distribution is unlimited.	

13. ABSTRACT (Maximum 200 words)

A signal (if present) is located somewhere in a band of frequencies characterized by a total of N search bins. The signal occupies an arbitrary set of $\underline{M}$ of these bins, where not only is $\underline{M}$ unknown, but also, the locations of the particular $\underline{M}$ occupied bins are unknown. Also, the signal strength is unknown.

A class of processors, called the power-law processors, is investigated, in which the available data is raised to the ν-th power prior to summation over all data values. The required threshold settings for achieving false alarm probabilities in the range down to 1E-6 have been determined for power values $\nu = 2, 3, 2.5$. The receiver operating characteristics have been determined and plotted, for these same values of power ν, for a wide range of values of $\underline{M}$. These results allow for accurate extraction of required signal-to-noise ratios to achieve a specified level of performance, as measured by the false alarm and detection

14. SUBJECT TERMS		15. NUMBER OF PAGES
Detection Power-Law Processor Unknown structure	Likelihood Ratio Unknown Location Unknown Extent	92
		16. PRICE CODE

17. SECURITY CLASSIFICATION OF REPORT	18. SECURITY CLASSIFICATION OF THIS PAGE	19. SECURITY CLASSIFICATION OF ABSTRACT	20. LIMITATION OF ABSTRACT
Unclassified	Unclassified	Unclassified	SAR

13. ABSTRACT (continued)

probabilities, P_f and P_d.

One of the most surprising and pleasant results of this study is the discovery that the power-law processor with $\nu = 2.5$ performs near optimum, even without any knowledge of the number of occupied bins $\underline{M}$, or the average signal power per bin, $\underline{S}$. This conclusion has been drawn only upon the numerical example of $N = 1024$, and for probabilities P_f, P_d in the range between the low-quality operating point $1E-3, .5$ and the high-quality operating point $1E-6, .9$.

TABLE OF CONTENTS

LIST OF FIGURES

LIST OF TABLES

LIST OF SYMBOLS

N	total number of search bins
$\underline{M}$	actual number of bins occupied by signal
$\underline{L}$	actual set of locations of the occupied bins
$\underline{S}$	actual average signal power per bin
H_0	hypothesis 0, noise-only present
H_1	hypothesis 1, signal and noise present
bold	random variable
$\mathbf{x}_n$	n-th observation, bin output, data input, (1)
q_0	probability density function of $\mathbf{x}_n$ under H_0, (1)

q_1	probability density function of x_n under H_1, (2)
$\underline{a}$	strength parameter, (3)
p_0	joint probability density function of $\{x_n\}$ under H_0, (4)
K	binomial coefficient $(N|\underline{M})$, (5), (7)
L_k	k-th occupancy set, (5)
p_1	joint probability density function of $\{x_n\}$ under H_1, (5)
LR	likelihood ratio, (6)
$\underline{w}$	weighting coefficient, (7)
X_k	k-th linear sum of data $\{x_n\}$ over set L_k, (7)
v	fixed threshold, (8)
Q_2	quadratic sum of X_k, (12)
T_ν	sum of data to the ν-th power, (13), (20), (31)
a,b	auxiliary coefficients for Q_2, (14), (15)
Q_3	cubic sum of X_k, (17)
a,b,c	auxiliary coefficients for Q_3, (18), (19)
z	decision variable, (21), (29), (31)
y_n	auxiliary random variable, (21), (29), (31)
$f_y(\xi)$	characteristic function of y_n under H_1, (22)
overbar	ensemble average, (22)
w( )	error function of complex argument, (22)
$f_y^0(\xi)$	characteristic function of y_n under H_0, (24)
$f_z^0(\xi)$	characteristic function of z_n under H_0, (24)
$f_z(\xi)$	characteristic function of z_n under H_1, (25)
P_f	false alarm probability, (26)
P_d	detection probability, (28)
$\bar{z}$	mean of z, (30)

DETECTION PERFORMANCE OF POWER-LAW PROCESSORS FOR RANDOM SIGNALS OF UNKNOWN LOCATION, STRUCTURE, EXTENT, AND STRENGTH

INTRODUCTION

This technical report is the third of a series of four NUWC technical reports by this author, covering the following topics:

(a) modified generalized likelihood ratio processors,

(b) generalized likelihood ratio processors,

(c) power-law processors, and

(d) optimum processing,

respectively. Topic (a) was completed in [1], resulting in a substantial compilation of receiver operating characteristics for the breakpoint modification considered there. Topic (b) was addressed in [2], again resulting in numerous receiver operating characteristics that quantify the performance of the modification called the sum-of-M-largest processor. The overall goal of the extended investigation is to determine classes of processors that perform at or near optimum levels of performance and that can be easily realized, analyzed, and assessed, even in these situations of scant knowledge about the detailed signal characteristics. The reader should be familiar with the earlier material before undertaking the current analyses and results.

In this report, we will derive the form of the optimum processor in this environment, and then simplify it to the point of realizing an alternative simple robust processor, namely the class of power-law processors. This power-law class will not require or use information such as the average signal-to-noise

ratio per bin, $\underline{S}$, or the number of bins, $\underline{M}$, occupied by signal (when present); this is consistent with the fact that such information is not available in practical applications anyway.

Some previous results on the performance of power-law processors, topic (c), have been reported in [3] and [4]. However, they considered detection of a Gaussian burst signal in Gaussian noise, whereas our input data have exponential probability density functions. Also, they did not consider very small values of $\underline{M}/N$, where N is the total number of search bins in which the signal could lie; we will address cases of $\underline{M}$ varying all the way from $\underline{M} = 1$ to $\underline{M} = N = 1024$. Their processor was arrived at in an ad hoc fashion, whereas ours is derived as an approximation to the optimum processor. Finally, they did not compare the performance of their power-law processors with any absolute bound on performance; we will undertake and complete that latter task in a future technical report treating topic (d) mentioned above.

Although the previous authors couched their signal as a contiguous burst of $\underline{M}$ samples in time [4; page 210, above (1)], they never used this fact for deriving an optimum processor, nor in the ad hoc processor they adopted. Thus, their results actually apply to the broader class of signals whose occupancy pattern in time (or frequency) is completely unknown. The optimum processor for contiguous bursts would utilize this contiguous knowledge and perform significantly better by virtue of being able to reduce the size of the search problem considerably. This case of increased signal information is not addressed here in this technical report either.

PROBLEM DEFINITION

The search space consists of N (frequency) bins, each containing independent identically-distributed noises of unit power. This situation is presumed to be accomplished by an earlier normalization procedure. The number N is under our control and is always a known quantity. When signal is absent, hypothesis H_0, the probability density function of each of the bin output noises is completely known.

When signal is present, hypothesis H_1, the quantity $\underline{M}$ is the actual number of bins occupied by the signal; this is frequently an unknown parameter. The quantity $\underline{L}$ is the actual set of bins occupied by signal, when signal is present; for example, if $\underline{M} = 4$, then we might have for the occupied set, $\underline{L} = \{2,3,7,29\}$, meaning that bins 2,3,7,29 have signal in them. This quantity $\underline{L}$ is always unknown in our investigation. Finally, the quantities $\{\underline{S}_n\}$ are the actual average signal powers in the n-th bin in occupied set $\underline{L}$, when signal is present; these average signal powers are unknown. We shall presume here that all the actual signal powers per bin are equal to a common (unknown) value $\underline{S}$ in the occupied set of bins $\underline{L}$, and zero elsewhere.

PROBABILITY DENSITY FUNCTIONS OF INDIVIDUAL BIN OUTPUTS

We now specify the detailed character of the probability density functions of the input data, namely p_0 and p_1, under hypotheses H_0 and H_1, respectively. In both hypotheses, the bin outputs or observations $\{x_n\}$ are taken as the squared envelopes of the outputs of (disjoint) narrowband filters subject to a Gaussian input random process; alternatively, the observations can be interpreted as the magnitude-squared outputs of a fast Fourier transform subject to a Gaussian input process. It is assumed that these bin outputs (random variables) $\{x_n\}$ are statistically independent of each other, which is consistent with a frequency-disjoint requirement.

Since the bin output noise has been normalized at unit level, the probability density function of the n-th observation x_n is, under hypothesis H_0, an exponential of the form

$$q_0(u_n) = \exp(-u_n) \quad \text{for } u_n > 0 \, , \quad 1 \leq n \leq N \, . \tag{1}$$

On the other hand, when signal is present, hypothesis H_1, with signal power $\underline{S}$ per bin, the density of x_n is changed to

$$q_1(u_n) = \underline{a} \exp(-\underline{a}\, u_n) \quad \text{for } u_n > 0 \, , \quad n \, \varepsilon \, \underline{L} \, , \tag{2}$$

where we have defined the strength parameter

$$\underline{a} = \frac{1}{1 + \underline{S}} \, . \tag{3}$$

Observe that the actual signal power per bin, $\underline{S}$, can also be

4

interpreted as the actual signal-to-noise power ratio per bin, since the noise power per bin has been normalized at unity.

PROBABILITY DENSITY FUNCTIONS OF THE SET OF OBSERVATIONS

The probability density function governing the complete observation $\{x_n\}$ under hypothesis H_0 follows from (1) and the statistical independence of $\{x_n\}$ as

$$p_0(u_1,\ldots,u_N) = \prod_{n=1}^{N} \{\exp(-u_n)\} . \tag{4}$$

Under hypothesis H_1, the signal can land in any set of $\underline{M}$ disjoint bins, out of the total of N search bins. This results in a total number of possibilities $K = (N|\underline{M})$, the latter quantity being the binomial coefficient. Furthermore, each set occurs with equal probability 1/K. Thus, there are K occupancy sets, each of size $\underline{M}$, namely $\{L_k\}$ for $1 \leq k \leq K$. The probability density function governing the observation $\{x_n\}$ is therefore

$$p_1(u_1,\ldots,u_N) = \sum_{k=1}^{K} \left[\frac{1}{K} \prod_{n \epsilon L_k} \{\underline{a} \exp(-\underline{a}u_n)\} \prod_{n \ell L_k} \{\exp(-u_n)\} \right] , \tag{5}$$

where we used (1) and (2).

DERIVATION OF OPTIMUM PROCESSOR

We initiate the investigation of optimum signal processing and detection by presuming, for the time being, that the number of bins, $\underline{M}$, occupied by signal (when present), and the common average signal power per bin, $\underline{S}$, are both known, but that the specific locations, $\underline{L}$, of the bins occupied by signal are completely unknown. This will enable us to derive the optimum processor in this environment.

Then, we will simplify this complicated time-consuming likelihood ratio procedure, eliminating the dependence on the parameters $\underline{M}$ and $\underline{S}$ in the proce; this is consistent with the practical situation, where these parameters are unknown. The resulting approximations will turn out to yield the class of power-law processors, which will occupy most of the succeeding analysis and performance prediction.

The likelihood ratio for observation $\{x_n\}$ is, from (4) and (5), the random variable

$$\text{LR} \equiv \frac{p_1(x_1, \ldots, x_N)}{p_0(x_1, \ldots, x_N)} = \frac{1}{K} \underline{a}^{\underline{M}} \sum_{k=1}^{K} \left[\prod_{n \varepsilon L_k} \{\exp(x_n[1 - \underline{a}])\} \right] =$$

$$= \frac{1}{K} \underline{a}^{\underline{M}} \sum_{k=1}^{K} \exp\left(\underline{w} \, X_k \right) , \tag{6}$$

where we have defined

$$\underline{w} \equiv 1 - \underline{a} = \frac{S}{1 + \underline{S}} , \quad X_k \equiv \sum_{n \varepsilon L_k} x_n \quad \text{for } 1 \leq k \leq K = \binom{N}{\underline{M}} . \tag{7}$$

7

The likelihood ratio test is therefore

$$\sum_{k=1}^{K} \exp\left(\underline{w}\ X_k\right) \underset{<}{>} v\ , \tag{8}$$

where v is a fixed threshold. The likelihood ratio test indicates to compute <u>all</u> K possible linear sums $\{X_k\}$ in (7), each of size $\underline{M}$, weight each by common value $\underline{w}$, exponentiate each term, and sum over all the possible K sets. For large N, the integer K is very large; then, (8) is a very time-consuming impractical prescription and requires knowledge of $\underline{S}$, which is very unlikely.

SPECIAL CASES

As a special case, for $\underline{M} = 1$, then $K = (N|1) = N$, and (7) and (8) reduce to

$$\sum_{n=1}^{N} \exp(\underline{w}\ x_n) \underset{<}{>} v\ . \tag{9}$$

This optimum processor can be easily realized if $\underline{S}$ is known; it can also be readily simulated in order to determine its performance.

At the other extreme, for the special case of $\underline{M} = N$, then $K = (N|N) = 1$, and (7) and (8) become

$$\exp\left(\underline{w}\ \sum_{n=1}^{N} x_n\right) \underset{<}{>} v\ , \quad \text{or equivalently,} \quad \sum_{n=1}^{N} x_n \underset{<}{>} v\ , \tag{10}$$

where the latter v is a different threshold value, of course.

This processor, called the energy detector, does not require knowledge of $\underline{S}$ or $\underline{M}$. It has already been analyzed, and receiver operating characteristics have been obtained [1; pages 21 - 22 and 81 - 90].

QUADRATIC SIMPLIFICATION OF LIKELIHOOD RATIO TEST

In an attempt to simplify the likelihood ratio test (8), suppose we approximate exponential function exp(x) by quadratic function $\alpha + \beta x^2$ over the range of typical arguments x likely to be encountered. The quadratic does not emphasize the very large arguments as much as the exponential does, but it does give more importance to larger arguments than a linear function would. (The cubic alternative $\alpha + \beta x^3$ will be considered below.)

When we substitute the quadratic approximation into (8), there follows

$$\sum_{k=1}^{K} \exp\left(\underline{w}\ X_k\right) \cong \sum_{k=1}^{K} \left(\alpha + \beta\ \underline{w}^2\ X_k^2\right) = K\ \alpha + \beta\ \underline{w}^2 \sum_{k=1}^{K} X_k^2 \ . \quad (11)$$

The corresponding approximate likelihood ratio test is therefore simply

$$Q_2 \equiv \sum_{k=1}^{K} X_k^2 \underset{<}{\overset{>}{\ }} v \ , \quad (12)$$

where we have discarded all the data-independent factors that we can. A very important feature of test (12) is that knowledge of

average signal power per bin, $\underline{S}$, is not required for its realization. However, knowledge of $\underline{M}$ is still required for test (12). Also, K can be too large to make test (12) practical.

In order to simplify (12) further, we expand each and every linear sum X_k in (12) in terms of its particular $\underline{M}$ components x_n according to set L_k in (7). We also define the data power sum

$$T_\nu \equiv \sum_{n=1}^{N} x_n^\nu , \qquad (13)$$

where ν need not be integer. Then, after some manipulation, expansion of (12) yields the identity

$$Q_2 = \binom{N-1}{\underline{M}-1} \left(a\, T_2 + b\, T_1^2 \right) , \qquad (14)$$

where coefficients

$$a = \frac{N-\underline{M}}{N-1} , \qquad b = \frac{\underline{M}-1}{N-1} ; \qquad a + b = 1 . \qquad (15)$$

For $\underline{M} = 1$, a is 1, while b is zero; thus, Q_2 in (14) is then composed solely of the <u>quadratic</u> sums of the data $\{x_n\}$, namely T_2; see (13). Conversely, for $\underline{M} = N$, a is zero, while b is 1; that is, Q_2 in (14) is then converted over to the square of a sum of <u>linear</u> terms in the data $\{x_n\}$, namely T_1. In between these two extreme values of $\underline{M}$, the changeover in the data-dependent part of Q_2 is linear in $\underline{M}$ for both coefficients a and b, as indicated by (15). Thus, there is a smooth transition in Q_2 in (14), from using only squared terms to using only linear terms in the data $\{x_n\}$, as $\underline{M}$ varies from 1 to N.

10

CUBIC SIMPLIFICATION OF LIKELIHOOD RATIO TEST

On the other hand, if we use the cubic function $\alpha + \beta x^3$ as an approximation to the exponential function $\exp(x)$, then (8) can be developed as follows:

$$\sum_{k=1}^{K} \exp\left(\underline{w} \, X_k\right) \approx \sum_{k=1}^{K} \left(\alpha + \beta \, \underline{w}^3 \, X_k^3\right) = K \, \alpha + \beta \, \underline{w}^3 \sum_{k=1}^{K} X_k^3 \; . \tag{16}$$

The corresponding approximate likelihood ratio test is then

$$Q_3 \equiv \sum_{k=1}^{K} X_k^3 \; \underset{<}{\overset{>}{}} \; v \; . \tag{17}$$

Although simpler than original test (8), test (17) still requires too many terms to make it practical.

Again, as above, we substitute for each term X_k in (17), its linear composition (7) in terms of data $\{x_n\}$, and expand out all the cubic terms. The result is, after considerable manipulation, the identity

$$Q_3 = \binom{N-1}{\underline{M}-1} \left(a \, T_3 + b \, T_2 \, T_1 + c \, T_1^3\right) \; , \tag{18}$$

where coefficients

$$a = \frac{N-\underline{M}}{N-1} \frac{N-2\underline{M}}{N-2} \; , \qquad b = 3 \frac{M-1}{N-1} \frac{N-\underline{M}}{N-2} \; , \qquad c = \frac{M-1}{N-1} \frac{M-2}{N-2} \; . \tag{19}$$

For $\underline{M} = 1$, we have $a = 1$, $b = 0$, $c = 0$; thus, sum Q_3 in (18) is then composed solely of <u>cubic</u> terms in the data $\{x_n\}$,

according to T_3 in (13). Conversely, for $\underline{M} = N$, we find $a = 0$, $b = 0$, $c = 1$; that is, sum Q_3 is then converted over to the cube of a sum T_1 involving only <u>linear</u> terms in the data $\{x_n\}$. In between these two extreme values of $\underline{M}$, the changeover in the data-dependent part of Q_3 is quadratic in $\underline{M}$ for all three coefficients a, b, c. Coefficient b reaches its peak at $\underline{M} = (N+1)/2$, with a value approximately 3/4, while c is about 1/4 there. A list of values of the coefficients a, b, c at select values of $\underline{M}$ is given below. We always have $a + b + c = 1$, as may be verified from (19).

VALUES OF COEFFICIENTS

$\underline{M}$	a	b	c
1	1	0	0
2	$\dfrac{N-4}{N-1}$	$\dfrac{3}{N-1}$	0
$\dfrac{N}{2}$	0	$\dfrac{3}{4}\dfrac{N}{N-1}$	$\dfrac{1}{4}\dfrac{N-4}{N-1}$
$\dfrac{N+1}{2}$	$\dfrac{1}{2}\dfrac{-1}{N-2}$	$\dfrac{3}{4}\dfrac{N-1}{N-2}$ (max)	$\dfrac{1}{4}\dfrac{N-3}{N-2}$
$\dfrac{3}{4}N$	$\dfrac{-N^2/8}{(N-1)(N-2)}$ (min)	$\dfrac{9}{16}\dfrac{N(N-4/3)}{(N-1)(N-2)}$	$\dfrac{9}{16}\dfrac{(N-4/3)(N-8/3)}{(N-1)(N-2)}$
N	0	0	1

OBSERVATIONS ON DATA PROCESSING

The cubic-approximation results in (18) and (19) show that
the optimum processor indicates a gradual transition from
emphasis on cubed data, through squared data, to linear data, as
$\underline{M}$ is increased from 1 to N. Coupled with the similar result for
the quadratic approximation in (14) and (15), this suggests that
one should consider the use of sum T_{ν} in (13), for general ν, as
the decision variable and as a possible candidate for near-
optimum processing as $\underline{M}$ varies.

It should be observed that some rather drastic approximations
have been adopted in the extraction of T_{ν} as a candidate decision
variable. First, the exponential function in (8) has been
replaced by either a quadratic or a cubic function. Then, the
resulting terms have been expanded out and collected in a
particular power form. Finally, the behaviors of the
coefficients of these power forms have been used in a heuristic
fashion to deduce the power-law processor.

The best choice of ν is an open question at this point,
as is the specific degradation incurred by resorting to the
approximation T_{ν} as the decision variable, instead of using the
optimum likelihood ratio test (8). Analytical and/or simulation
comparisons of (8) and T_{ν} must be conducted in order to ascertain
the exact degradations in performance that accompany the various
alternative approximations to the optimum likelihood ratio test,
and to determine the best value(s) of ν to use for minimum
degradation.

The use of power sum T_ν in (13) as the decision variable is very attractive from a computational viewpoint. It involves only N calculations, not K, which are extremely simple if ν is an integer, like 1 or 2 or 3. Other intermediate (non-integer) values of ν would take longer. Also, no knowledge of M or S is required to realize the approximate likelihood ratio test

$$T_\nu = \sum_{n=1}^{N} x_n^\nu \underset{<}{\overset{>}{}} v \ . \tag{20}$$

This is called the class of power-law processors, and will be the major topic of numerical investigation here.

For $\nu = 1$, the power-law processor corresponds to the energy detector [1; pages 21 - 22]. On the other hand, as $\nu \to \infty$, power-law processor (20) tends towards the maximum processor; that is, the performance of (20) tends towards that of $\max\{x_1,\ldots,x_N\}$. This maximum processor has already been thoroughly analyzed and quantified in the study on the sum-of-M-largest processor in [2], when M = 1 there.

The power-law nature of test (20) emphasizes the stronger samples in the given data $\{x_n\}$ over the weaker ones, in making its decision about signal presence or absence when the occupied set of bins, L, is completely unknown; recall that the data $\{x_n\}$ can be interpreted themselves as power quantities, being the envelope-squared outputs of narrowband filters. Also, in keeping with optimum test (8), approximate test (20) reaches its decision based upon a combination of all the data values $\{x_n\}$, and not upon a maximum of some subsets of the data.

ANALYSIS OF POWER-LAW PROCESSORS

We are interested in the performance of power-law processor
(20) when the statistics of the input data $\{x_n\}$ are given by (1)
and (2). The specific results for $\nu = 1$ are given by [1; pages
21 - 22 and 81 - 90], while the case of $\nu = \infty$, that is, the
maximum processor $\max\{x_1,\ldots,x_N\}$, is treated in [2; (30) - (33)
and tables 1 and 2].

QUADRATIC-LAW PROCESSOR

In this subsection, we consider the special case of $\nu = 2$,
for which we have the test

$$z \equiv T_2 = \sum_{n=1}^{N} x_n^2 \equiv \sum_{n=1}^{N} y_n \gtrless \nu \ . \tag{21}$$

Under hypothesis H_1, the characteristic function of the
individual random variable y_n is

$$f_y(\xi) \equiv \overline{\exp(i\xi y_n)} = \overline{\exp\left(i\xi x_n^2\right)} = \int_0^\infty du \ \underline{a} \ \exp(-\underline{a}u + i\xi u^2) =$$

$$= (1+i) \ \underline{a} \ \left(\frac{\pi}{8\xi}\right)^{\frac{1}{2}} w\left(\underline{a} \ \frac{-1+i}{(8\xi)^{\frac{1}{2}}}\right) \quad \text{for } \xi > 0 \ , \tag{22}$$

where we used (2) and the error function $w(z)$ of complex argument
[5; chapter 7]. An alternative expression for this character-
istic function, in terms of the real auxiliary functions f and g
defined in [5; 7.3.5 & 7.4.22 and 7.3.6 & 7.4.23], is given by

$$f_y(\xi) = \underline{a} \left(\frac{\pi}{2\xi}\right)^{\frac{1}{2}} \left[f\left(\frac{a}{(2\pi\xi)^{\frac{1}{2}}}\right) + i\ g\left(\frac{a}{(2\pi\xi)^{\frac{1}{2}}}\right)\right] \quad \text{for } \xi > 0 \ . \quad (23)$$

To complete the characteristic function, we have $f_y(0) = 1$ and $f_y(-\xi) = f_y(\xi)^*$, to complement the results in (22) and (23).

The characteristic function of y_n under hypothesis H_0 is obtained from (22) or (23) by setting average signal power $\underline{S}$ equal to 0, that is, by setting strength parameter $\underline{a}$ equal to 1; denote it by $f_y^O(\xi)$. Then, using the independence of input data $\{x_n\}$ in sum (21), the characteristic function of decision variable z under H_0 is

$$f_z^O(\xi) = \left(f_y^O(\xi)\right)^N \ . \quad (24)$$

On the other hand, the characteristic function of z under H_1 is given by

$$f_z(\xi) = \left(f_y^O(\xi)\right)^{N-\underline{M}} \left(f_y(\xi)\right)^{\underline{M}} \ , \quad (25)$$

where $\underline{M}$ is the actual number of bins containing signal. At this point, we have all the results we need in order to compute false alarm and detection probabilities of the quadratic-law processor in (21). The numerical method we employ, here and in the future sections of this report, is the accurate and efficient fast Fourier transform procedure for going directly from a given characteristic function to its exceedance distribution function, as given in [6].

The false alarm probability,

$$P_f = \text{Prob}(z > v | H_0) \, , \tag{26}$$

obtained through use of (22) and (24), is plotted versus threshold v in figure 1, for total search sizes N = 64, 128, 256, 512, 1024. The corresponding receiver operating characteristics for N = 1024 and for

$$\underline{M} = 1, 2, 3, 4, 8, 16, 32, 64, 128, 256, 512, 1024, \tag{27}$$

with average signal power per bin $\underline{S}$ (in decibels) as a parameter, are given in appendix A in figures A-1 through A-12, respectively. The detection probability, defined as

$$P_d = \text{Prob}(z > v | H_1) \, , \tag{28}$$

was obtained by use of (22) and (25).

Since these results used a very accurate computer routine for the complex error function $w(z)$, the false alarm probabilities in the 10^{-6} range are accurate, and the receiver operating characteristics are accurate over the complete range plotted. These plcts enable us to extract the required signal-to-nois2 ratio per bin to realize a specified level of performance, such as $P_f = 10^{-3}$, $P_d = 0.5$. For example, figure A-1 for N = 1024 and $\underline{M} = 1$ indicates that we must have the large value $\underline{S} = 14.8$ dB, whereas figure A-12 for N = 1024 and $\underline{M} = 1024$ requires the much smaller value $\underline{S} = -9.4$ dB, since the number of occupied bins, $\underline{M}$, is so much larger.
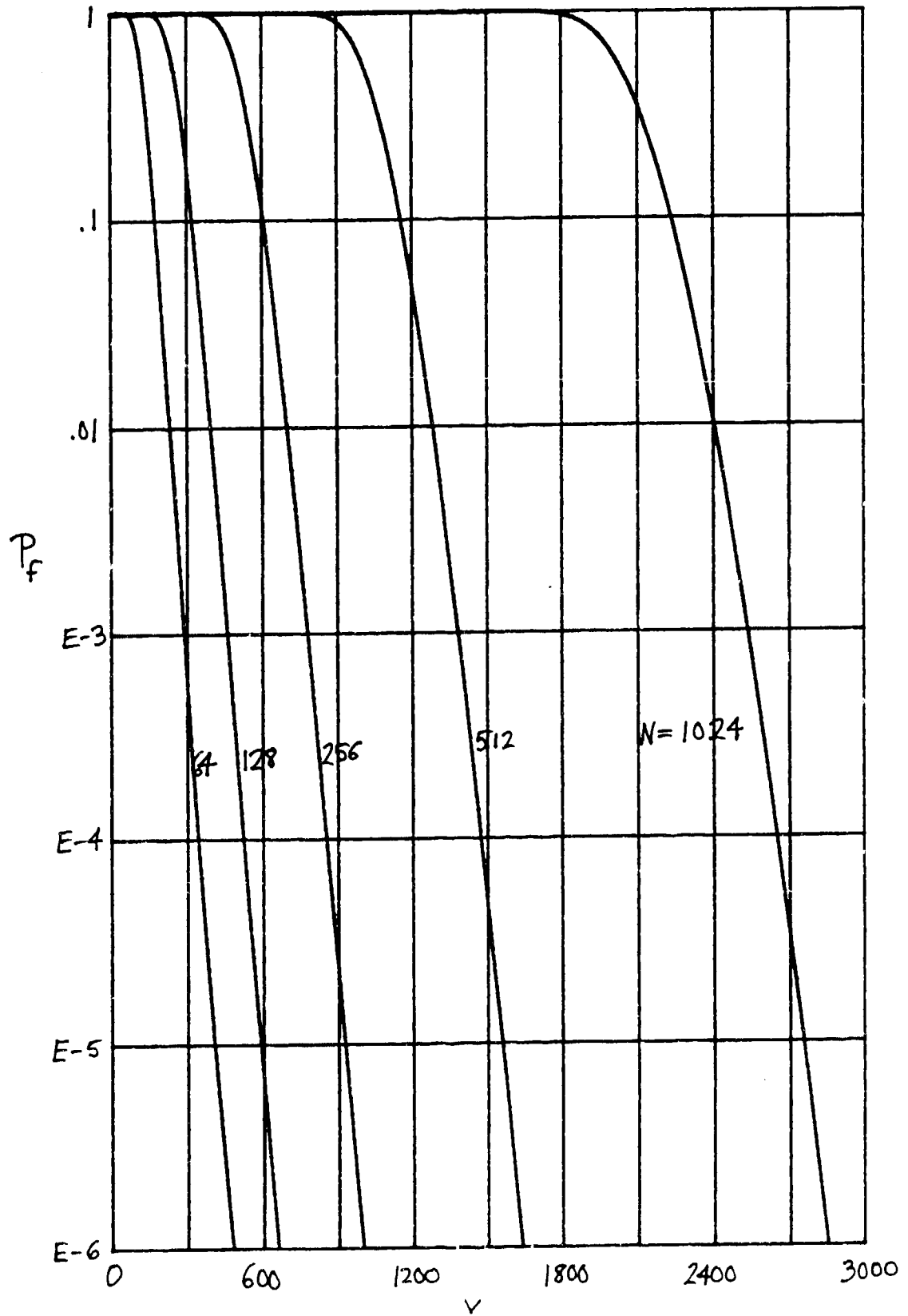
Figure 1.   False Alarm Probability for Quadratic-Law Processor

CUBIC-LAW PROCESSOR

Here, we consider the case of power law $\nu = 3$ in test (20), namely

$$z \equiv T_3 = \sum_{n=1}^{N} x_n^3 \equiv \sum_{n=1}^{N} y_n \overset{>}{\underset{<}{}} v \; . \tag{29}$$

Under hypothesis H_1, the characteristic function of an individual random variable y_n is

$$f_y(\xi) \equiv \overline{\exp(i\xi y_n)} = \overline{\exp\left[i\xi x_n^3\right]} = \int_0^\infty du \; \underline{a} \exp(-\underline{a}u + i\xi u^3) =$$

$$= \underline{a} \frac{\sqrt{3} + i}{2} \int_0^\infty dr \; \exp\left[-\xi r^3 - \underline{a}\frac{\sqrt{3}}{2}r - i \; \underline{a} \frac{r}{2}\right] \quad \text{for } \xi \geq 0 \; , \tag{30}$$

where we used (2). In order to obtain the latter integral form, we moved the contour in the u-plane to the radial line with angle $\pi/6$ radians and then made the change of variable $u = r \exp(i\pi/6)$.

The characteristic function of y_n under H_0, denoted by $f_y^o(\xi)$, follows from (30) by setting $\underline{a} = 1$ ($\underline{S} = 0$), and the characteristic function of decision variable z in (29) is again given by form (24). The lack of any computer routine for the complex function of ξ in (30) caused us to adopt the following numerical procedure. Integral (30) with $\underline{a} = 1$ ($\underline{S} = 0$) was accurately evaluated on the fine grid $\xi = 0(.001)3$ and stored. These values were then used in (24) to evaluate the characteristic function of z under hypothesis H_0, for values of $N = 64, 128, 256, 512, 1024$.

The numerical procedure in [6] was then employed to compute the false alarm probability, with the results given by figure 2. The curvature in the results at the 10^{-6} level are accurate, and are due to the cubic rule in (29).

The detection probability P_d could also have been obtained in a similar fashion, by using (30) with strength parameter $\underline{a} < 1$ ($\underline{S} > 0$). However, since we are generally interested in detection probability values in the neighborhood of 0.5 to 0.9, it was decided to avoid the bookkeeping, and to instead directly simulate test (29) for signal powers $\underline{S} > 0$. The results for $N = 1024$, and for the same $\underline{M}$ values as listed in (27), are given in figures B-1 through B-12 respectively, in appendix B. Each of these plots utilized at least 10,000 independent trials of random variable z in (29); thus, the receiver operating characteristics are very stable except for very small P_d values of no practical interest. There is sufficient stability to be able to accurately determine required signal-to-noise ratios to operate in the desired 0.5 to 0.9 range of detection probabilities.
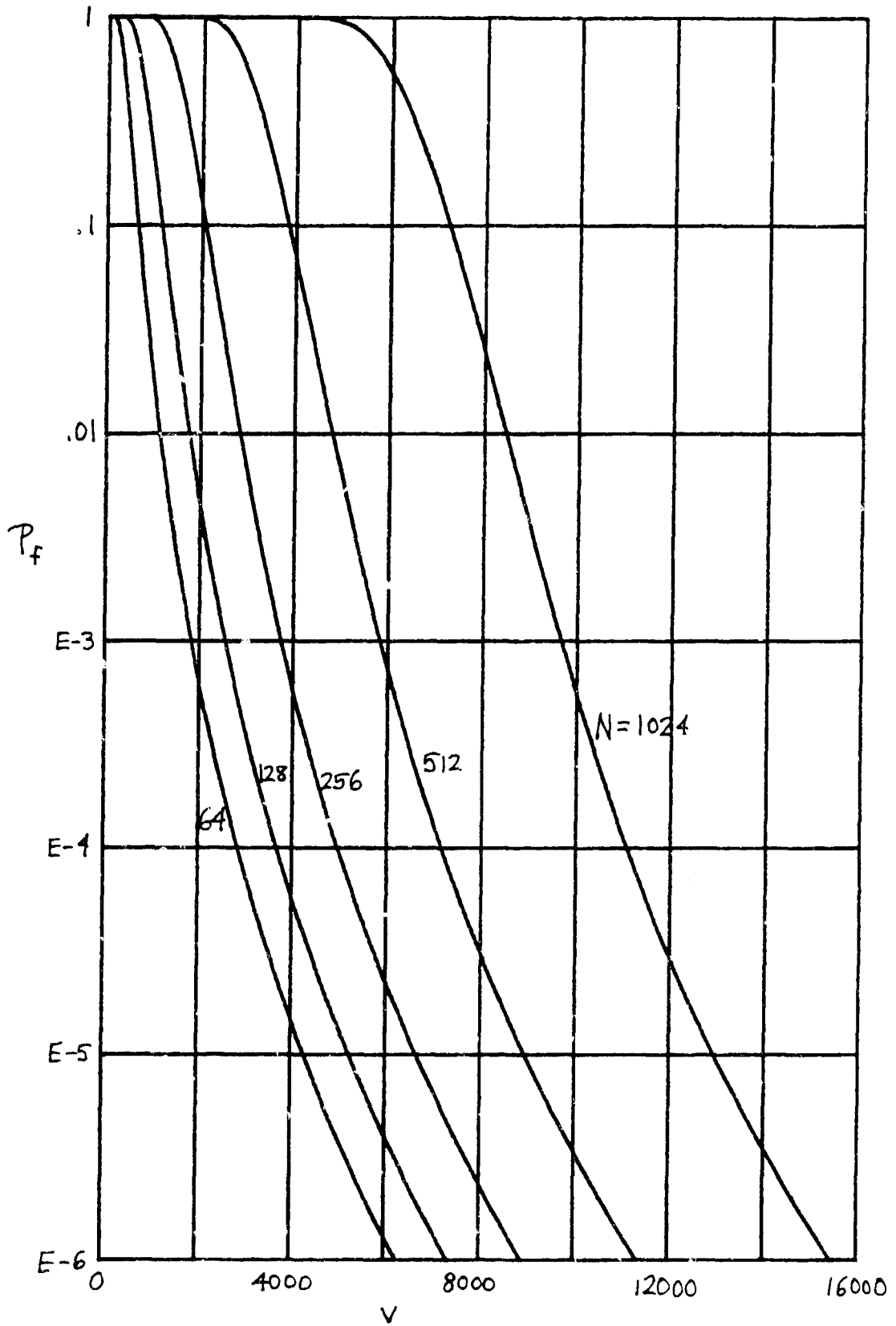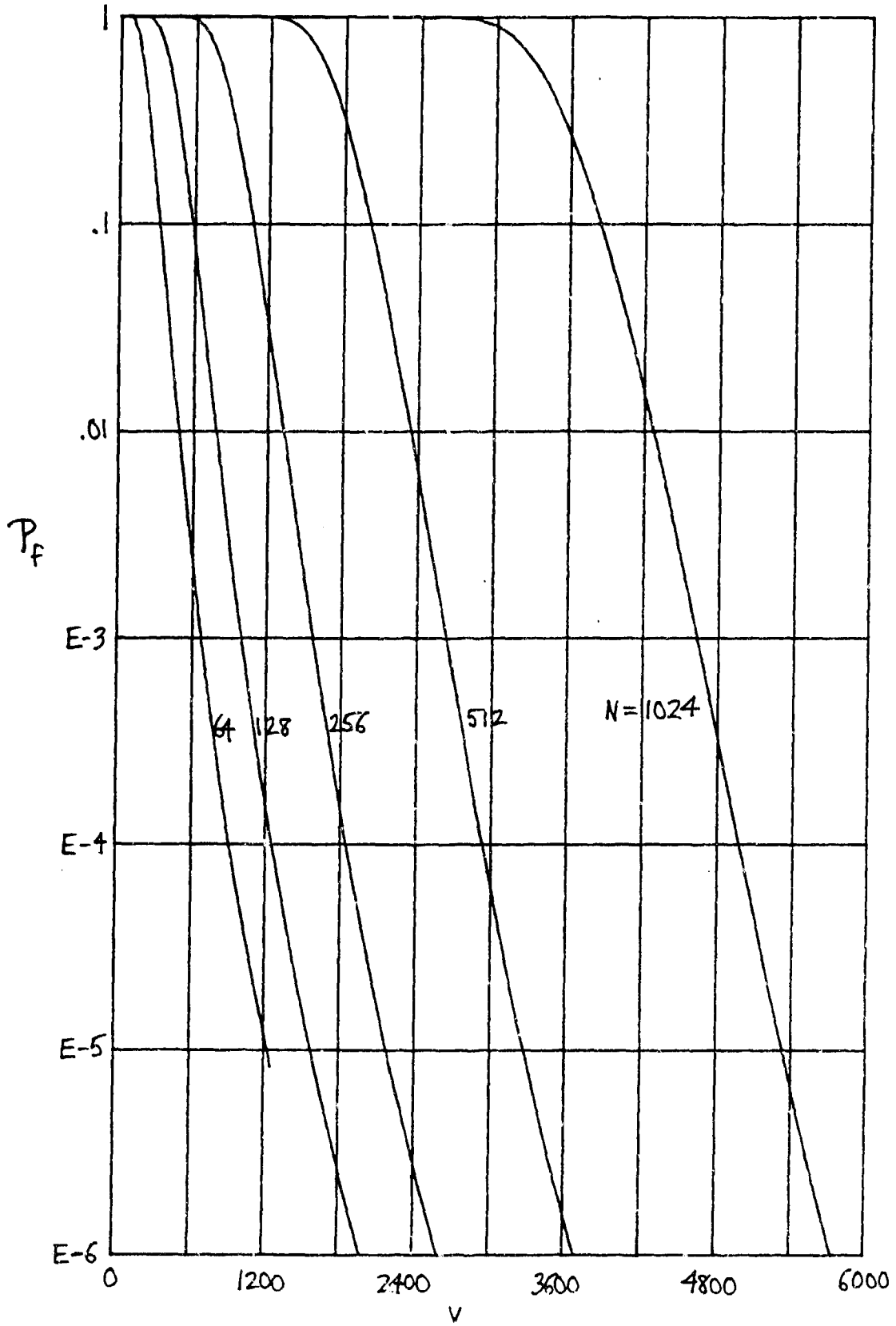
Figure 2.   False Alarm Probability for Cubic-Law Processor

GENERAL POWER-LAW PROCESSOR

The case of general power $\nu > 1$ in power-law test (20) is of interest here. That is, the decision variable is now

$$z \equiv T_\nu = \sum_{n=1}^{N} x_n^\nu \equiv \sum_{n=1}^{N} y_n \underset{<}{\overset{>}{}} v \, . \tag{31}$$

Under hypothesis H_0, the characteristic function of individual random variable y_n is, upon use of (1),

$$f_y^0(\xi) \equiv \overline{\exp(i\xi y_n)} = \overline{\exp\left(i\xi x_n^\nu\right)} = \int_0^\infty du \, \exp(-u + i\xi u^\nu) =$$

$$= \exp\left(\frac{i\pi}{2\nu}\right) \int_0^\infty dr \, \exp\left[-\xi r^\nu - \exp\left(\frac{i\pi}{2\nu}\right) r\right] \, . \tag{32}$$

Here, we moved the contour in the u-plane to the radial line with angle $\pi/(2\nu)$ radians and then made the change of variable $u = r \exp(i\pi/(2\nu))$. Since $\nu > 1$, the integral on r in (32) has more rapid decay than the integral on u; in addition, the oscillation of the integrand is constant with r, whereas it continually increases in the u integral.

The only case of (32) that was numerically investigated here was the choice $\nu = 2.5$; the reason for this selection will be seen later. The characteristic function in (32) was accurately numerically evaluated on the fine grid $\xi = 0(.001)3$ and stored. These values were then used in (24) to evaluate the characteristic function of z in (31) under hypothesis H_0, for

22

values of search size N = 64, 128, 256, 512, 1024. The numerical procedure in [6] was then employed to compute the false alarm probability, with the results given by figure 3. The only additional quantity required for [6] is the mean of decision variable z under hypothesis H_0, which is given by

$$\bar{z} = N \; \overline{x_n^\nu} = N \int_0^\infty du \; \exp(-u) \; u^\nu = N \; \Gamma(\nu+1) \; , \qquad (33)$$

and which equals N $\sqrt{\pi}$ 15/8 for ν = 2.5.

The detection probability P_d for power-law test (31), with ν = 2.5, was simulated for signal powers $\underline{S}$ > 0. The results for N = 10.4, and for the same $\underline{M}$ values as listed in (27), are given in figures C-1 through C-12 respectively, in appendix C. Each of these plots utilized at least 10,000 independent trials of random variable z in (31); thus, the receiver operating characteristics are very stable except for very small P_d values of no practical interest. There is sufficient stability to be able to accurately determine required signal-to-noise ratios to operate in the desired 0.5 to 0.9 range of detection probabilities.

Figure 3. False Alarm Probability for Power-Law Processor $\nu=2.5$

COMPARISON OF POWER-LAW PROCESSORS

The compilation of 36 receiver operating characteristics in appendices A, B, C, for ν = 2, 3, 2.5 respectively, prompts us to condense this information for easier interpretation and accessibility. To accomplish this, we define a low-quality operating point P_f = 10^{-3}, P_d = 0.5 and a high-quality operating point P_f = 10^{-6}, P_d = 0.9. We then read off the curves in the appendices the values of signal power $\underline{S}$(dB) which are required to realize these two levels of performance. These results are listed in tables 1 and 2, and are plotted in figures 4 and 5 for the low-quality and high-quality operating points, respectively, for $\underline{M}$ ranging over the set of values 1, 2, 3, 4, 8, 16, 32, 64, 128, 256, 512, 1024. The values of the power-law considered are ν = 1, 2, 2.5, 3, ∞. The results for ν = 1 and ν = ∞ come from [2; pages 40 - 41]. The ordinate, $\underline{M}\,\underline{S}$ in decibels, in figures 4 and 5 is actually the total signal power required in order to achieve the specified performance level. This total quantity is more meaningful and it condenses the range of ordinate values to a more manageable regime.

It is immediately seen that the best value of ν, to achieve minimum average signal power per bin $\underline{S}$, varies with the number of occupied signal bins, $\underline{M}$. For convenience, we confine the following discussion to the low-quality operating point depicted in figure 4. For example, if $\underline{M}$ = 1, the best value for ν is ∞, although ν = 3 is only 0.4 dB poorer. On the other hand, if $\underline{M}$ = 1024, the best ν is 1, but ν = 2 is only 0.5 dB poorer. In

between these extreme values of M, the best ν sweeps through all the intermediate values as M changes. This behavior is consistent with the earlier observations based upon approximations Q_2 in (14) and Q_3 in (18). Figures 4 and 5 constitute a numerical confirmation of the tenuous approximations that were employed in deriving (14) and (18), and in arriving at power-law test (20).

The reason for considering power-law value $\nu = 2.5$ is now clear from looking at the low-quality operating point results in figure 4. When M, the number of bins occupied by signal, is completely unknown, the best compromise value for ν is 2.5. This particular power-law processor performs about 1 dB poorer than the best in its class at the extreme values $M = 1$ and $M = 1024$; however, for intermediate values of M, it is close to the best in this class of processors.

On the other hand, for the high-quality operating point results in figure 5, perhaps the best power-law value is near $\nu = 2.25$. Numerical results for this case were not run; they can be found upon use of (32) and (33). However, for analytic simplicity and ease of practical realization, the quadratic-law processor $\nu = 2$ is recommended.

When the results in figures 4 and 5 are compared with the corresponding results for the modified generalized likelihood ratio processor in [1] and the sum-of-M-largest processor in [2; pages 42 - 48], the corresponding lower envelopes of required signal power are very close over the entire range of M from 1 to $N = 1024$. That is, the best performer in each class of processors requires about the same amount of signal power to

achieve the same level of performance.

However, there is one outstanding attribute of the power-law class that highly recommends it over the earlier two classes of processors, namely the modified generalized likelihood ratio processors [1] and the sum-of-M-largest processors [2]. The power-law processor, with ν fixed at value 2.5, does not need to know the value of M in order to perform near its best level. At the low-quality operating point for example, it loses no more than 1.2 dB with regard to the best level found thus far, regardless of the unknown value of M, the number of occupied signal bins. There is no need to guess at a breakpoint, x_o, or a number of terms, M, to use, as there was with the earlier processors; these choices could never be made intelligently without knowledge of M in the earlier processors.

This relative independence of the power-law class on M is a truly remarkable result and certainly could not have been anticipated from the debatable manipulations employed in arriving at the power-law class of processors. However, the question is still open as to the ultimate level of performance that can be attained by the optimum processor in this environment. That is, we would like to have an absolute lower bound on the curves in figures 4 and 5. This would tell us how good or bad the power-law class is, and whether we should bother to try to find yet another class of processors that performs still better. That problem is topic (d) mentioned previously on page 1; it has been solved and will be the subject of a future NUWC technical report [7] by this author.

Table 1. Required $\underline{S}$(dB) for $N = 1024$, $P_f = 10^{-3}$, $P_d = 0.5$

ν	1	2	2.5	3	∞
$\underline{M}$					
1	21.53	14.8	13.8	13.2	12.77
2	17.71	11.8	10.7	10.2	10.11
3	15.70	10.3	9.3	8.9	8.90
4	14.34	9.3	8.4	8.05	8.14
8	11.17	7.2	6.4	6.2	6.59
16	8.09	5.1	4.6	4.4	5.28
32	5.05	3.0	2.7	2.7	4.15
64	2.03	0.8	0.75	1.0	3.12
128	-0.98	-1.4	-1.3	-0.9	2.17
256	-3.99	-4.0	-3.6	-3.0	1.27
512	-7.00	-6.7	-6.1	-5.3	0.39
1024	-10.01	-9.4	-8.7	-7.8	-0.48

Table 2. Required $\underline{S}$(dB) for $N = 1024$, $P_f = 10^{-6}$, $P_d = 0.9$

ν	1	2	2.5	3	∞
$\underline{M}$					
1	31.81	24.0	23.2	23.0	22.92
2	24.85	18.1	17.3	17.1	17.29
3	21.73	15.6	14.75	14.7	15.09
4	19.77	14.1	13.3	13.3	13.82
8	15.61	11.0	10.4	10.5	11.45
16	11.94	8.3	7.95	8.2	9.70
32	8.56	6.0	5.8	6.2	8.31
64	5.34	3.7	3.8	4.3	7.17
128	2.22	1.4	1.7	2.5	6.18
256	-0.85	-1.0	-0.45	0.6	5.31
512	-3.89	-3.6	-2.8	-1.4	4.53
1024	-6.91	-6.3	-5.3	-3.6	3.81
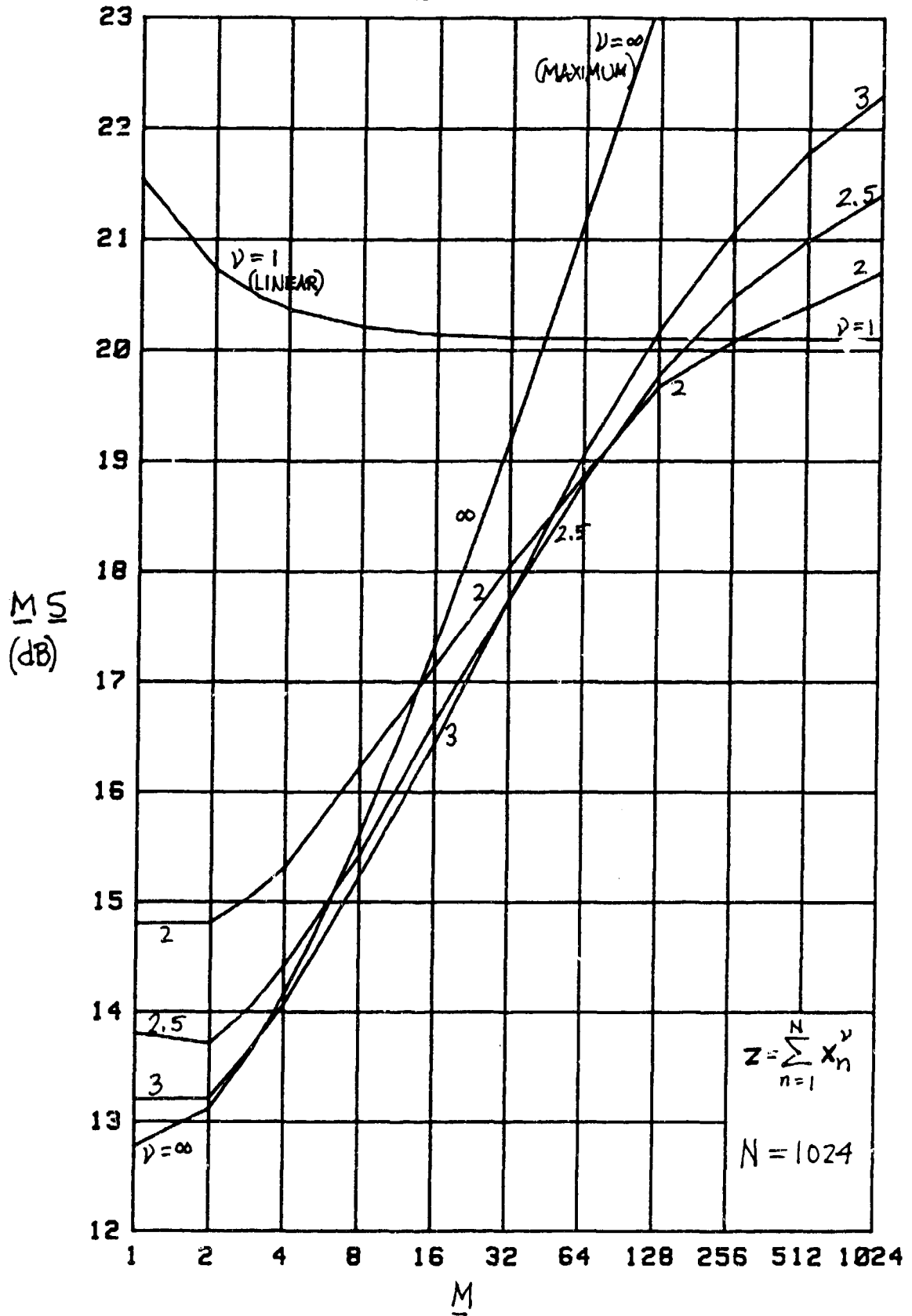
Figure 4. Required Total Signal Power for $P_f = 10^{-3}$, $P_d = 0.5$
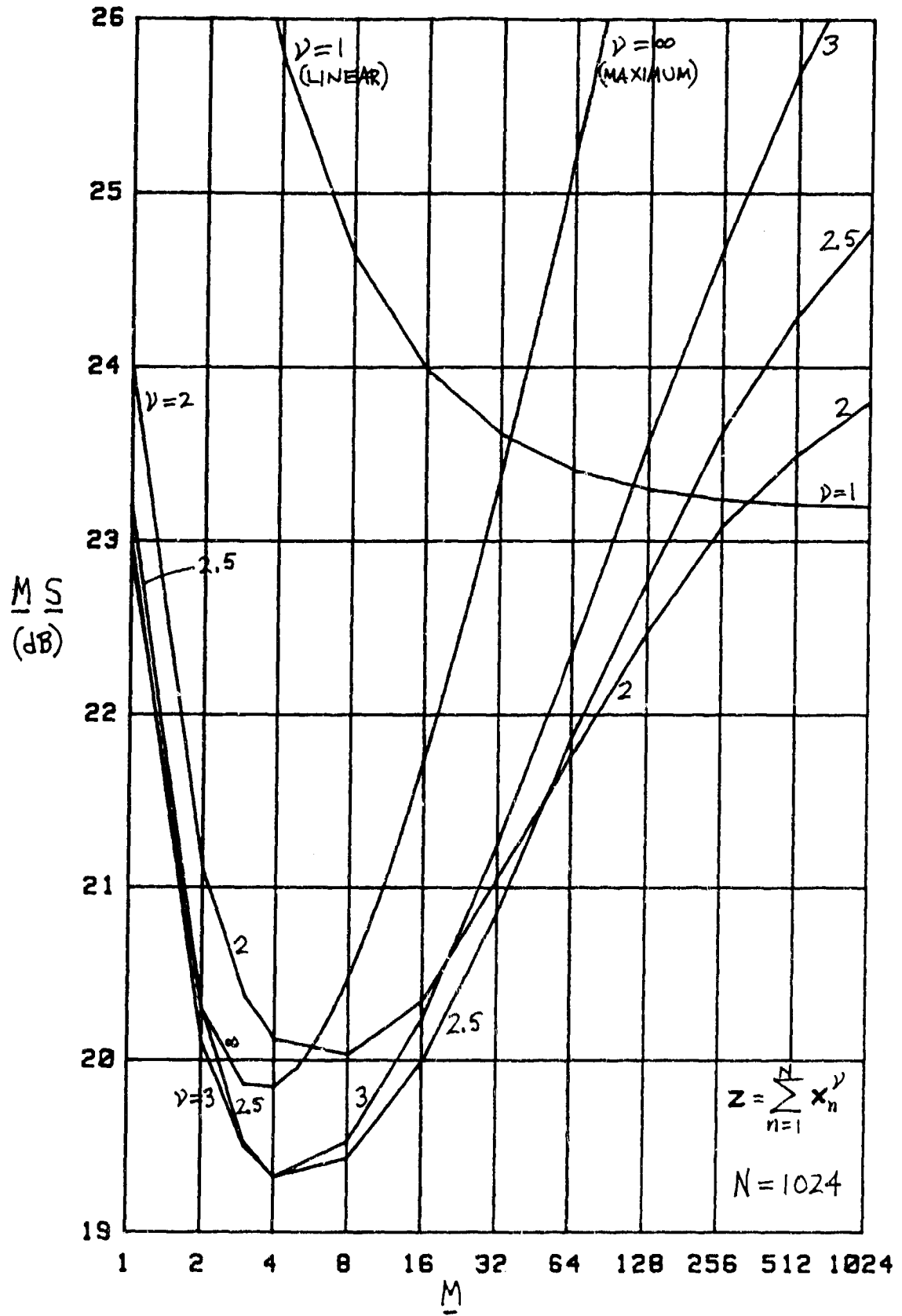
Figure 5. Required Total Signal Power for $P_f = 10^{-6}$, $P_d = 0.9$

SUMMARY

The class of power-law processors is characterized by raising each observed data point, x_n, to the ν-th power and summing over all the data points from 1 to N, regardless of the (unknown) value of M, the number of bins occupied by signal. The power-law processor can be regarded as a rough approximation to the optimum processor operating in this environment, trying to detect a signal without any structure.

The required threshold settings for achieving false alarm probabilities in the range down to 10^{-6} have been presented in figures 1, 2, 3 for power values $\nu = 2, 3, 2.5$, respectively. The receiver operating characteristics have been determined and plotted, for these same values of power ν, in appendices A, B, C respectively, for a wide range of values of M. These results allow for accurate extraction of required signal-to-noise ratios to achieve a specified level of performance, as measured by the false alarm and detection probabilities.

One of the most surprising and pleasant results of this study is the discovery that the power-law processor with $\nu = 2.5$ performs near optimum, even without any knowledge of the number of occupied bins M, or the average signal power per bin, S. This conclusion has been drawn only upon the numerical example of N = 1024, and for probabilities P_f, P_d in the range between the low-quality operating point $10^{-3}, 0.5$ and the high-quality operating point $10^{-6}, 0.9$. Additional ranges of numerical values have yet to be investigated.

The results in figure 5, for the required total signal power to achieve a specified level of performance, indicate an interesting behavior. Namely, there is a best division of the total power into approximately M = 4 or 5 bins, at which point the power-law processors with ν = 2.5 or 3 will achieve the specified performance with the minimum value 19.3 dB. However, this situation may not be achievable in the typical practical passive application where M, the number of occupied bins, is not under the receiver's control.

The greatest shortcoming of the results in this report is that the signal powers per bin have all been assumed equal in the occupied signal bins, with value S. An extension to allow for unequal arbitrary signal powers per bin, $\{S_n\}$, is clearly necessary and is underway. The power-law class will be the initial and primary candidate for signal detection in this situation. Also, a bound on performance, based perhaps on an argument analogous to that in [7], will be required to determine how close the power-law class is to optimum.

APPENDIX A.   RECEIVER OPERATING CHARACTERISTICS FOR $\nu = 2$

The decision variable z for this case is given by (21) as

$$z \equiv T_2 = \sum_{n=1}^{N} x_n^2 \underset{<}{\overset{>}{}} v \ . \qquad (A-1)$$

The characteristic functions of z under hypotheses H_0 and H_1 are given by (24) and (25), respectively, in conjunction with (22). The strength parameter $\underline{a} = (1 + \underline{S})^{-1}$, where $\underline{S}$ is the average signal power per bin. Twelve values of $\underline{M}$, the number of bins occupied by signal, have been considered; they are

$\underline{M} = 1, 2, 3, 4, 8, 16, 32, 64, 128, 256, 512, 1024,$ $\qquad$ (A-2)

and the corresponding receiver operating characteristics are plotted in figures A-1 through A-12, respectively. The curves are labeled by the parameter $\underline{S}(dB)$, which is equal to $10 \log_{10}(\underline{S})$. Thus, $\underline{S}(dB)$ can be interpreted as the required signal-to-noise ratio per bin in decibels. The total search size, N, is kept fixed at value 1024 for all these plots.
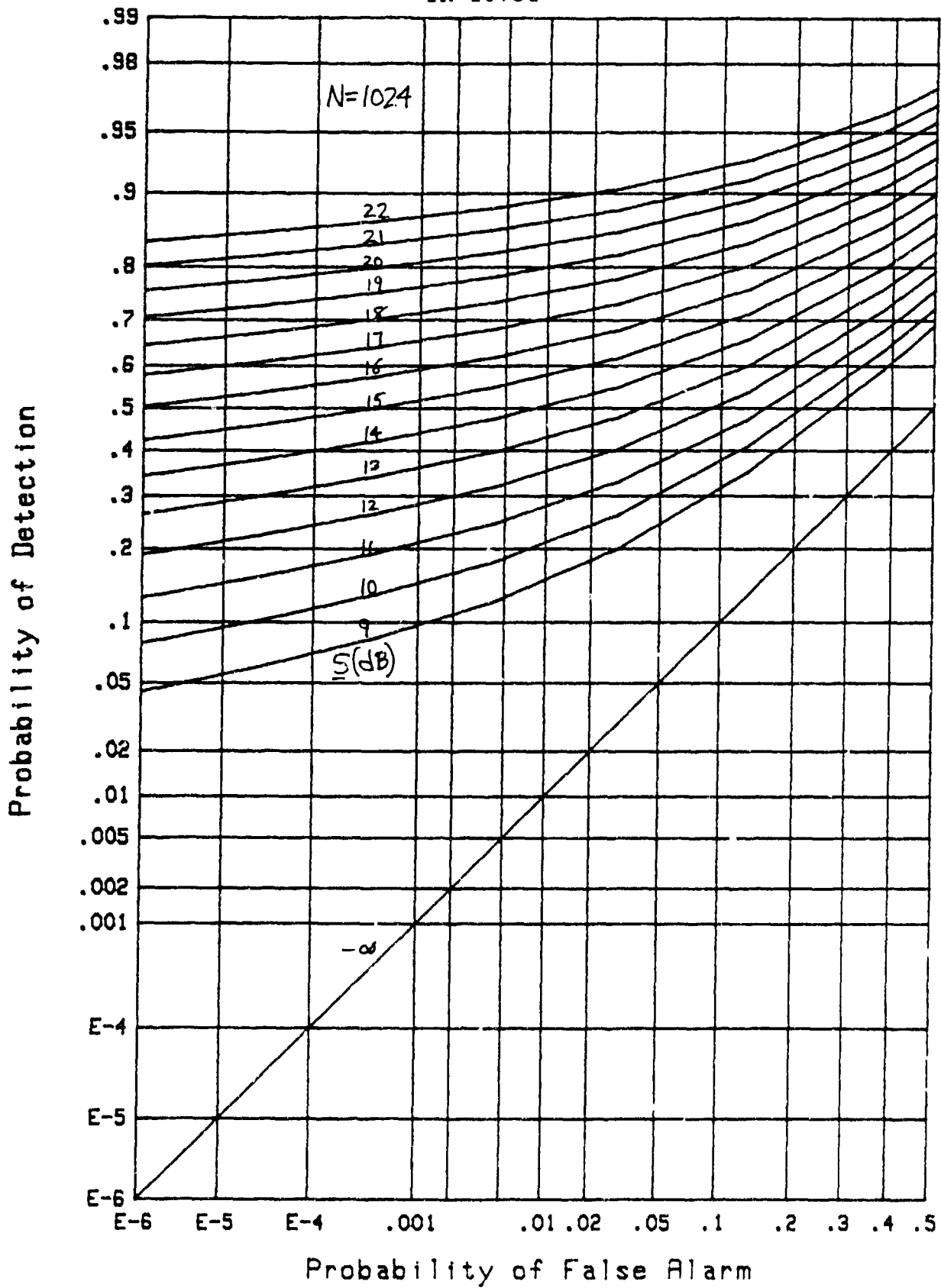
Figure A-1. Operating Characteristic for $\nu = 2$, $\underline{M} = 1$
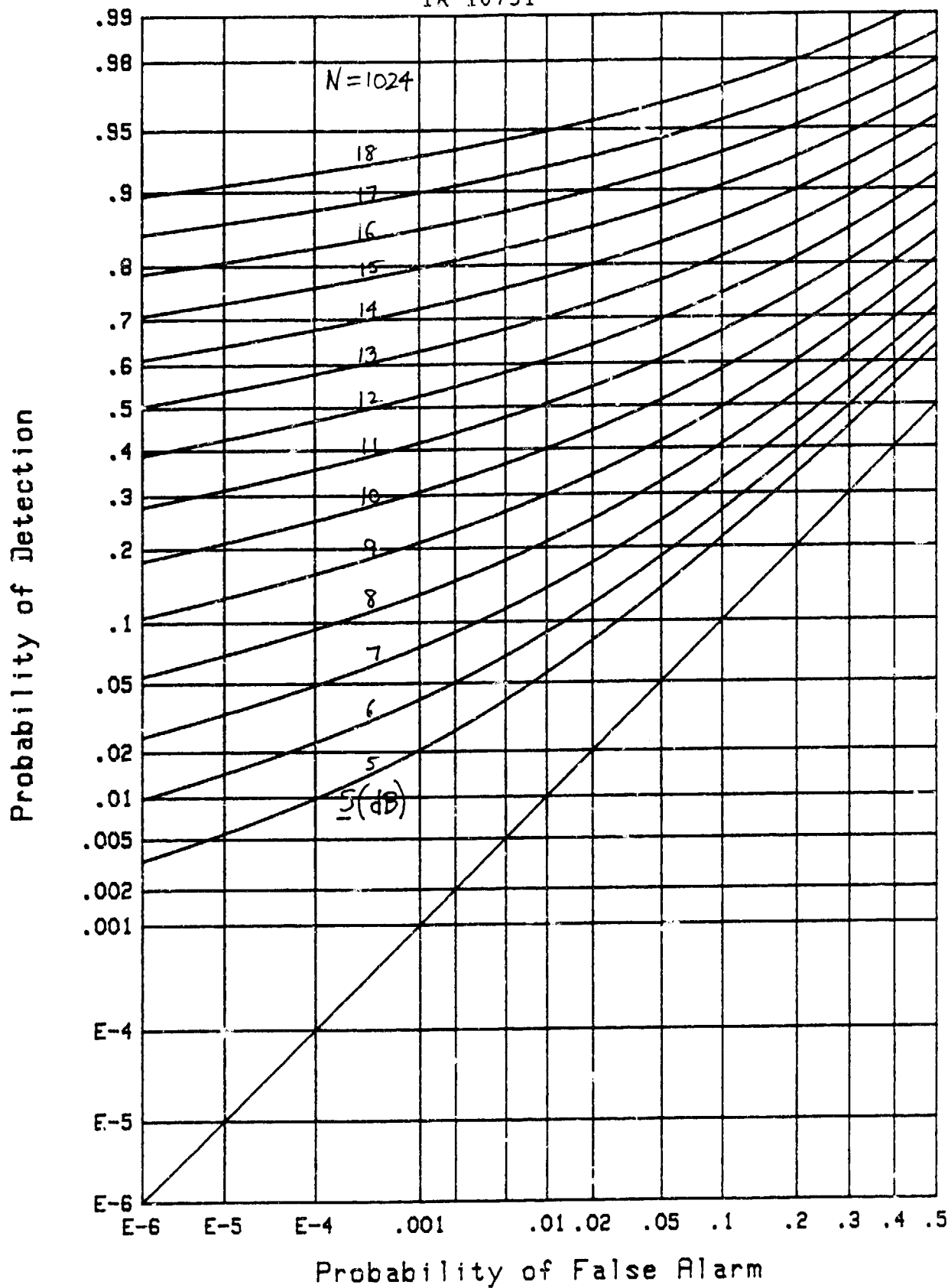
Figure A-2.   Operating Characteristic for $\nu = 2$, $\underline{M} = 2$
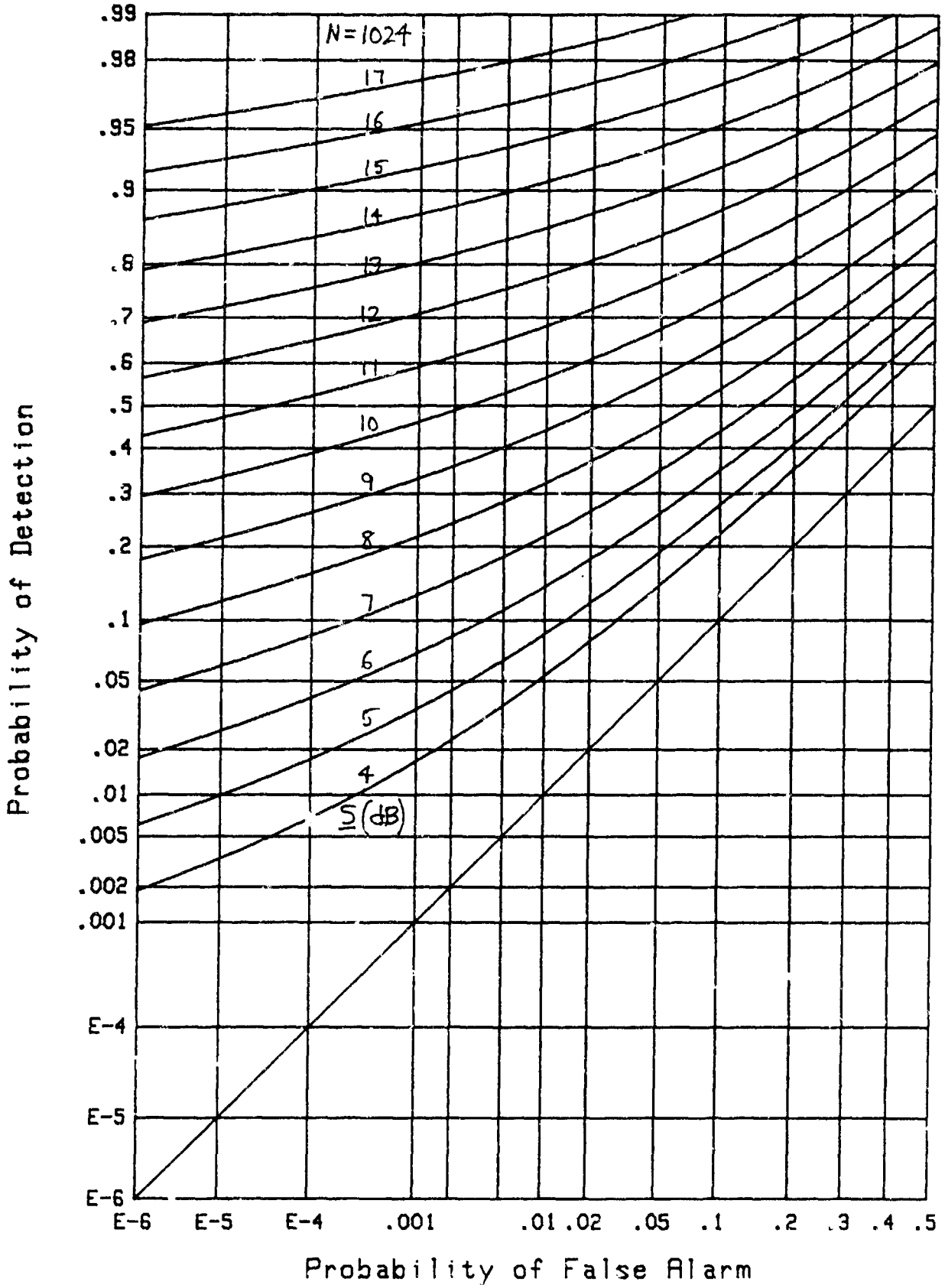
Figure A-3. Operating Characteristic for $\nu = 2$, $\underline{M} = 3$
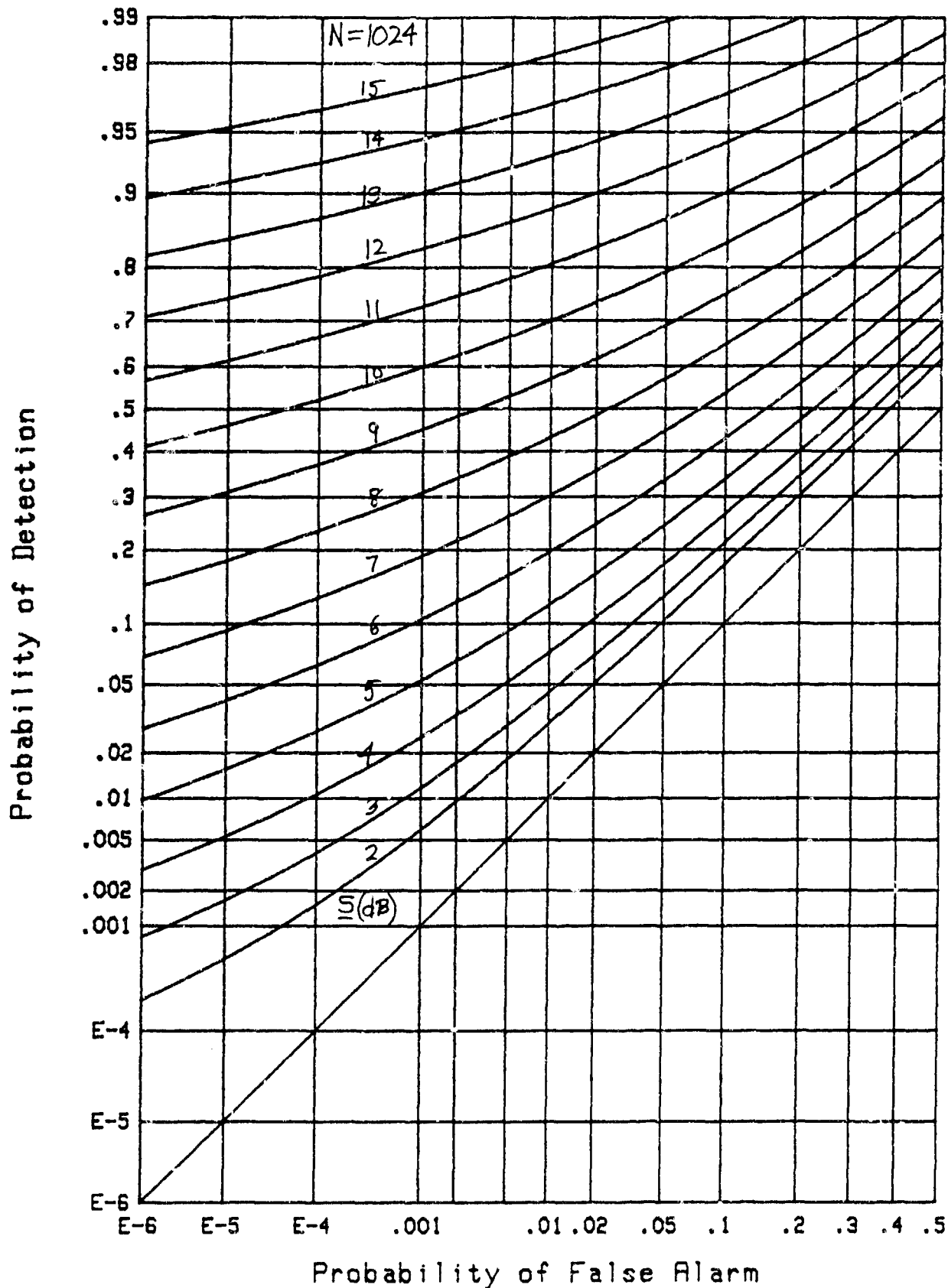
Figure A-4.   Operating Characteristic for $\nu = 2$, $\underline{M} = 4$
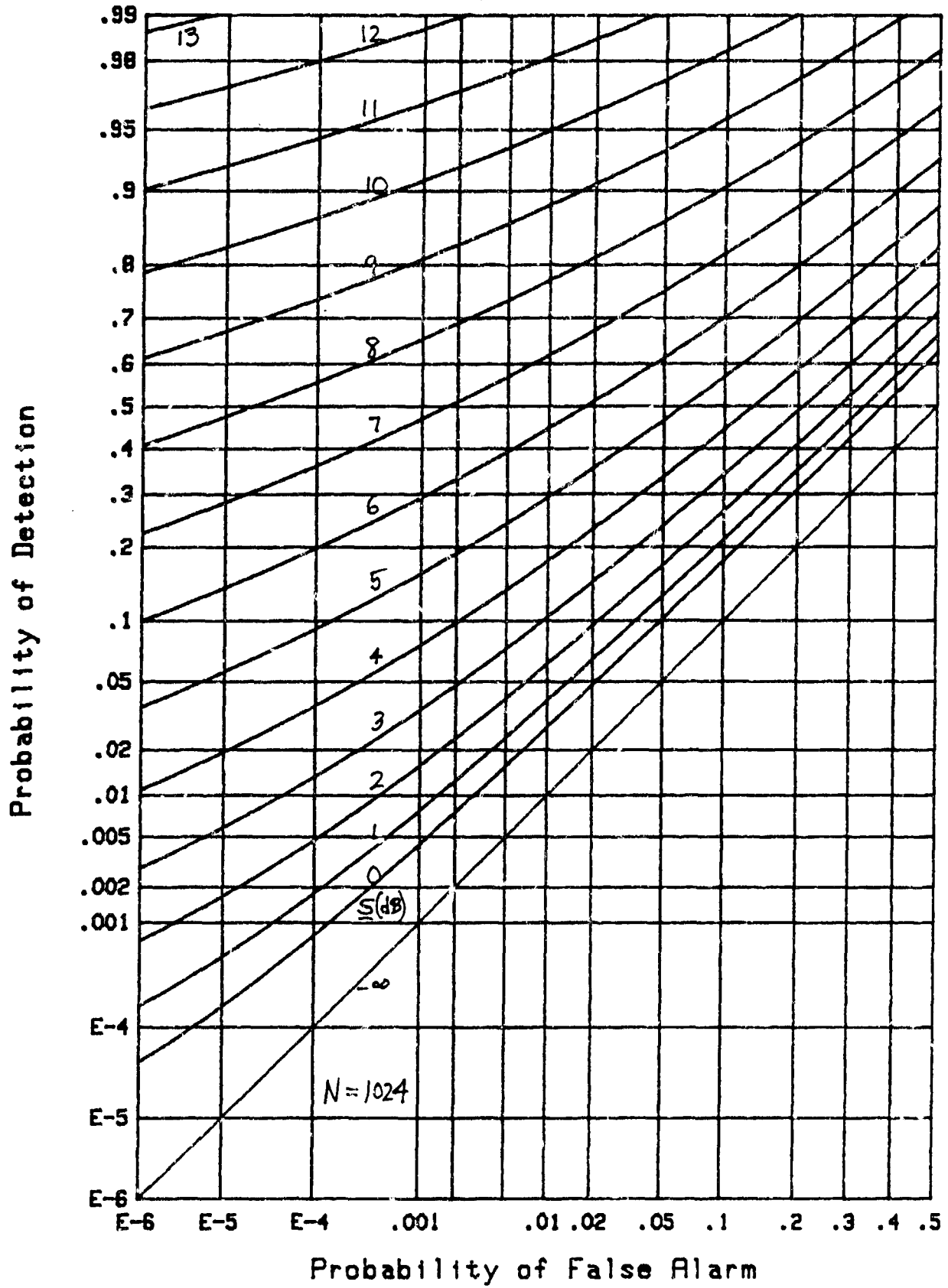
Figure A-5.   Operating Characteristic for $\nu = 2$, $\underline{M} = 8$
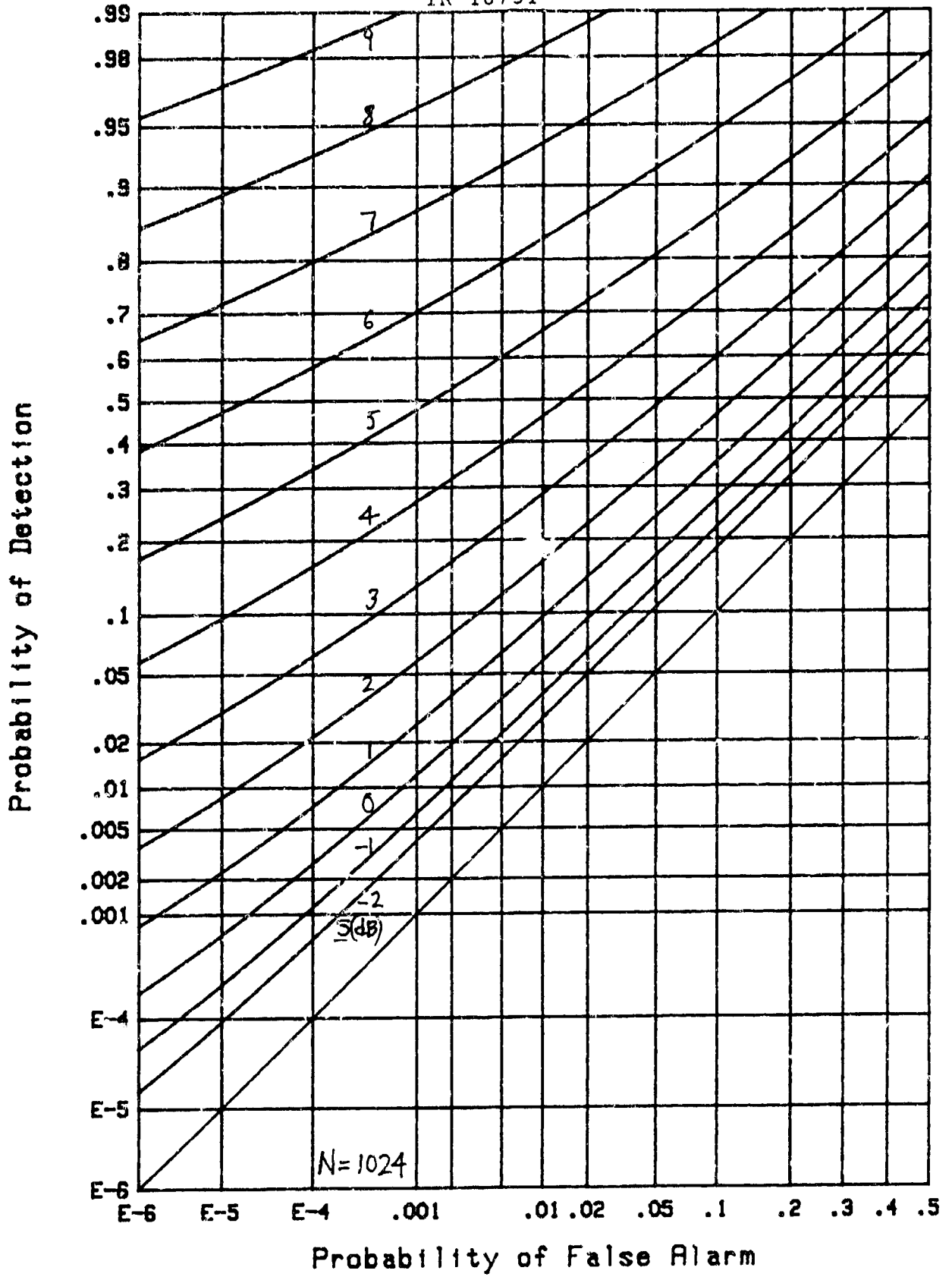
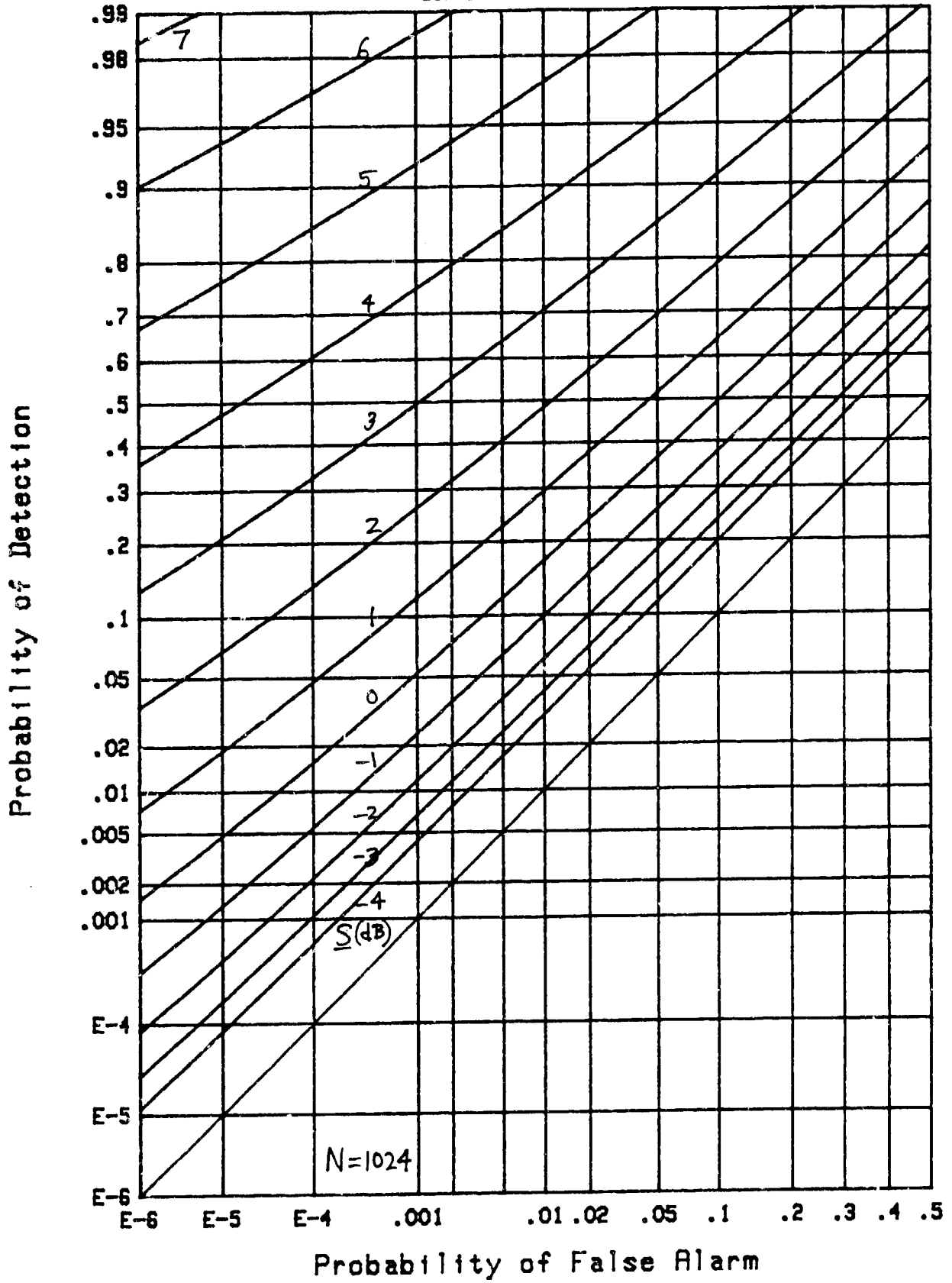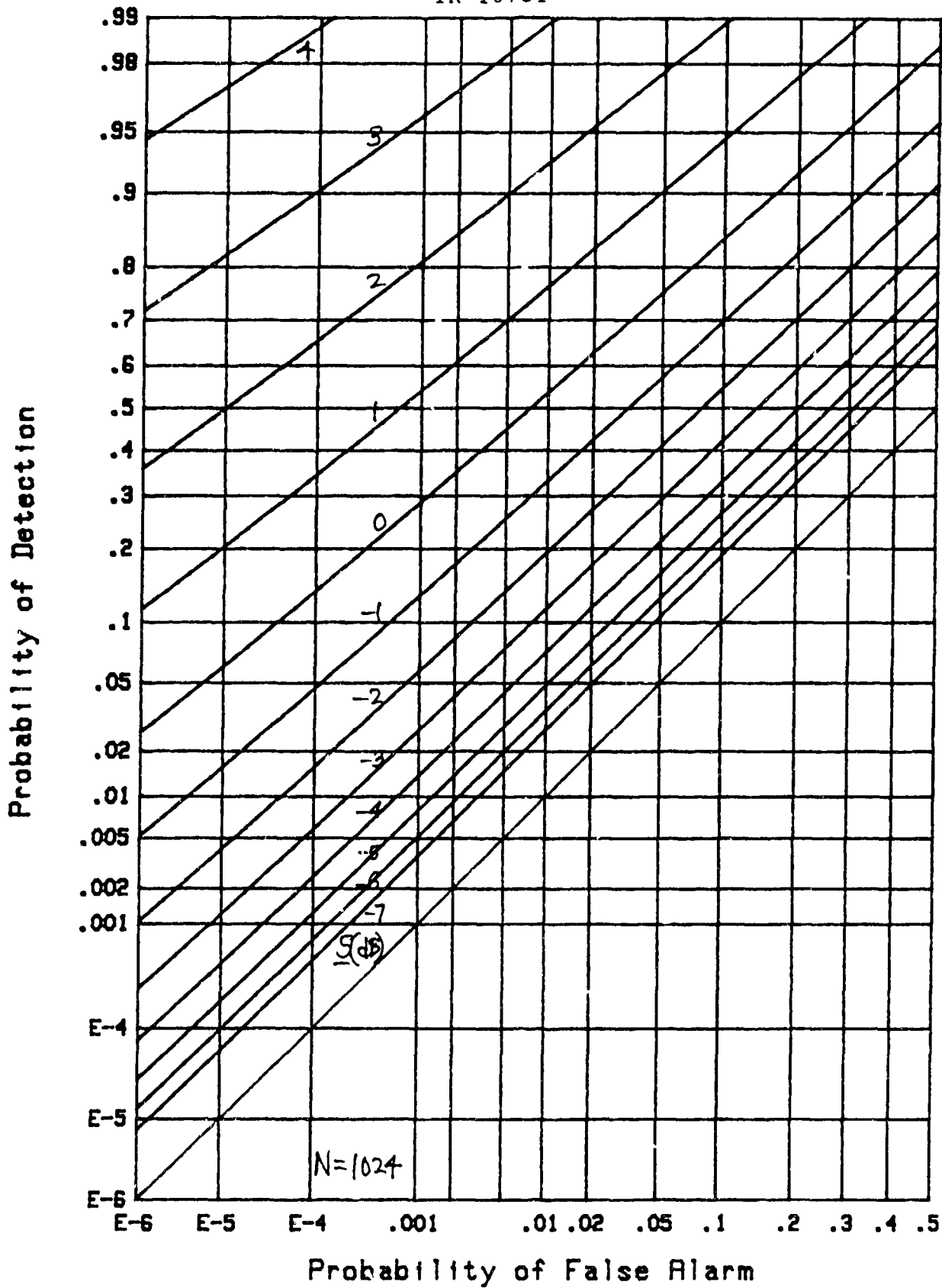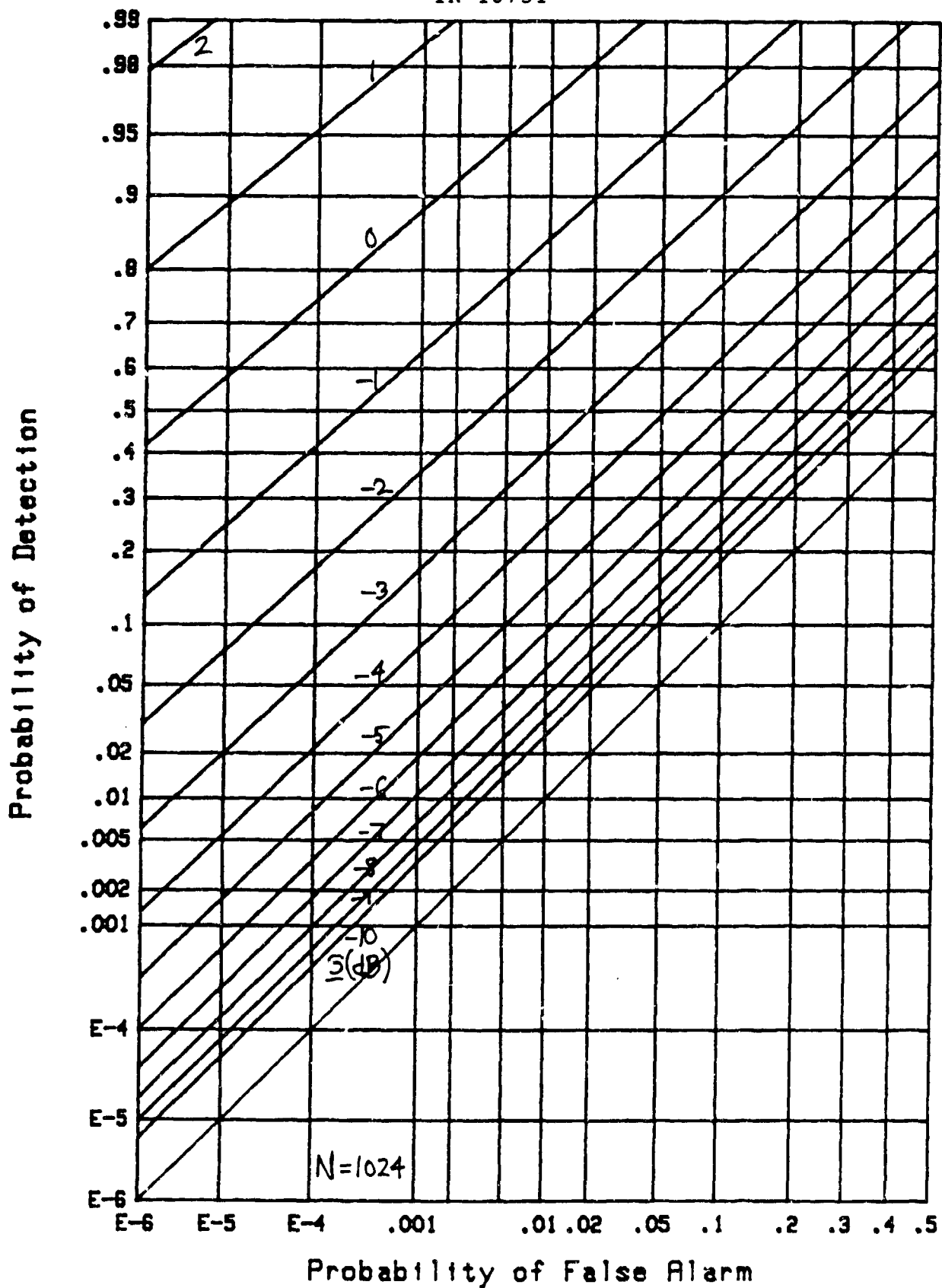Figure A-6.   Operating Characteristic for $\nu = 2$, $\underline{M} = 16$

Figure A-7.   Operating Characteristic for $\nu = 2$, $\underline{M} = 32$

Figure A-8. Operating Characteristic for $\nu = 2$, $\underline{M} = 64$

Figure A-9.   Operating Characteristic for $\nu = 2$, $\underline{M} = 128$
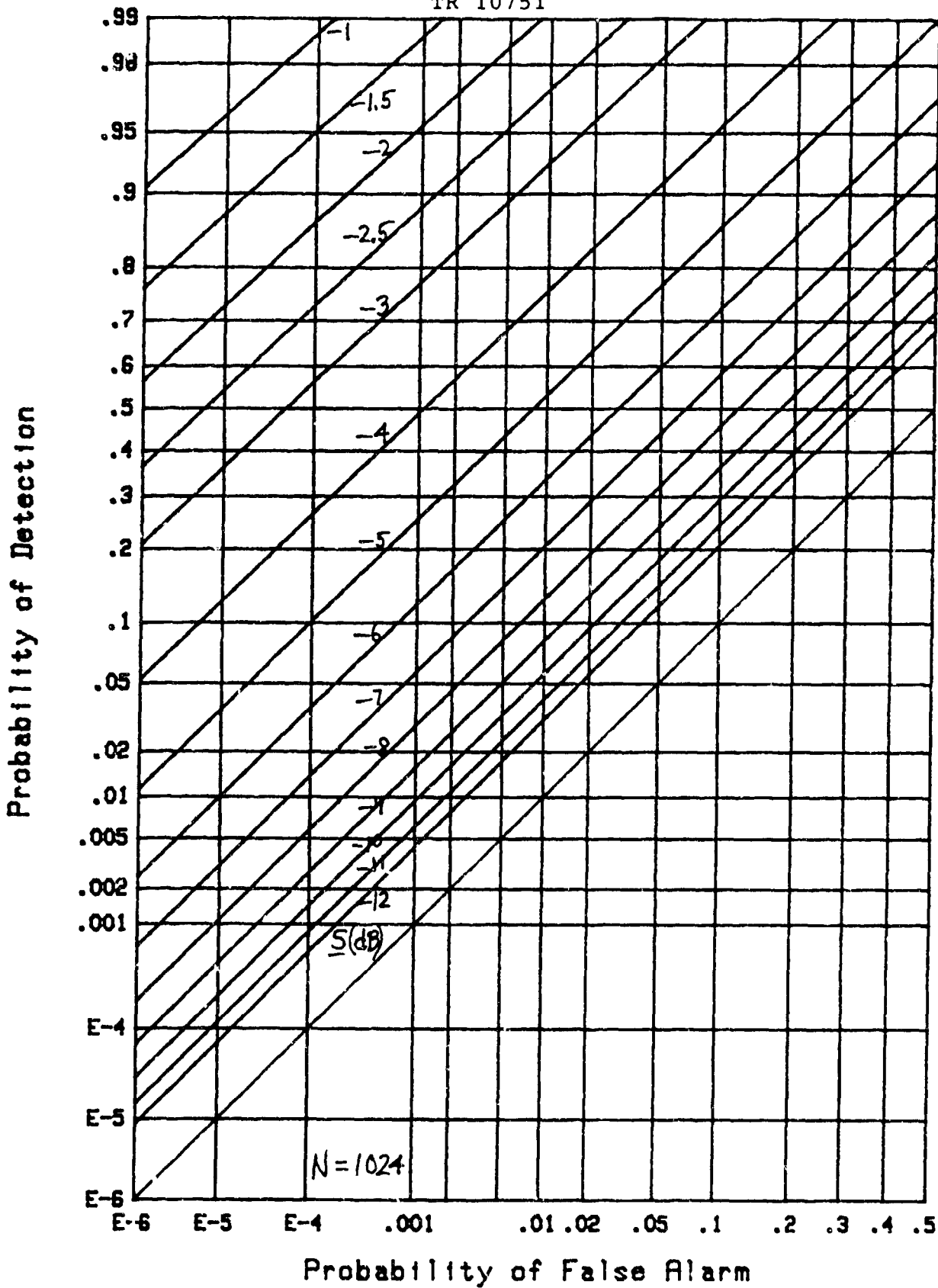
Figure A-10.   Operating Characteristic for $\nu = 2$, $\underline{M} = 256$
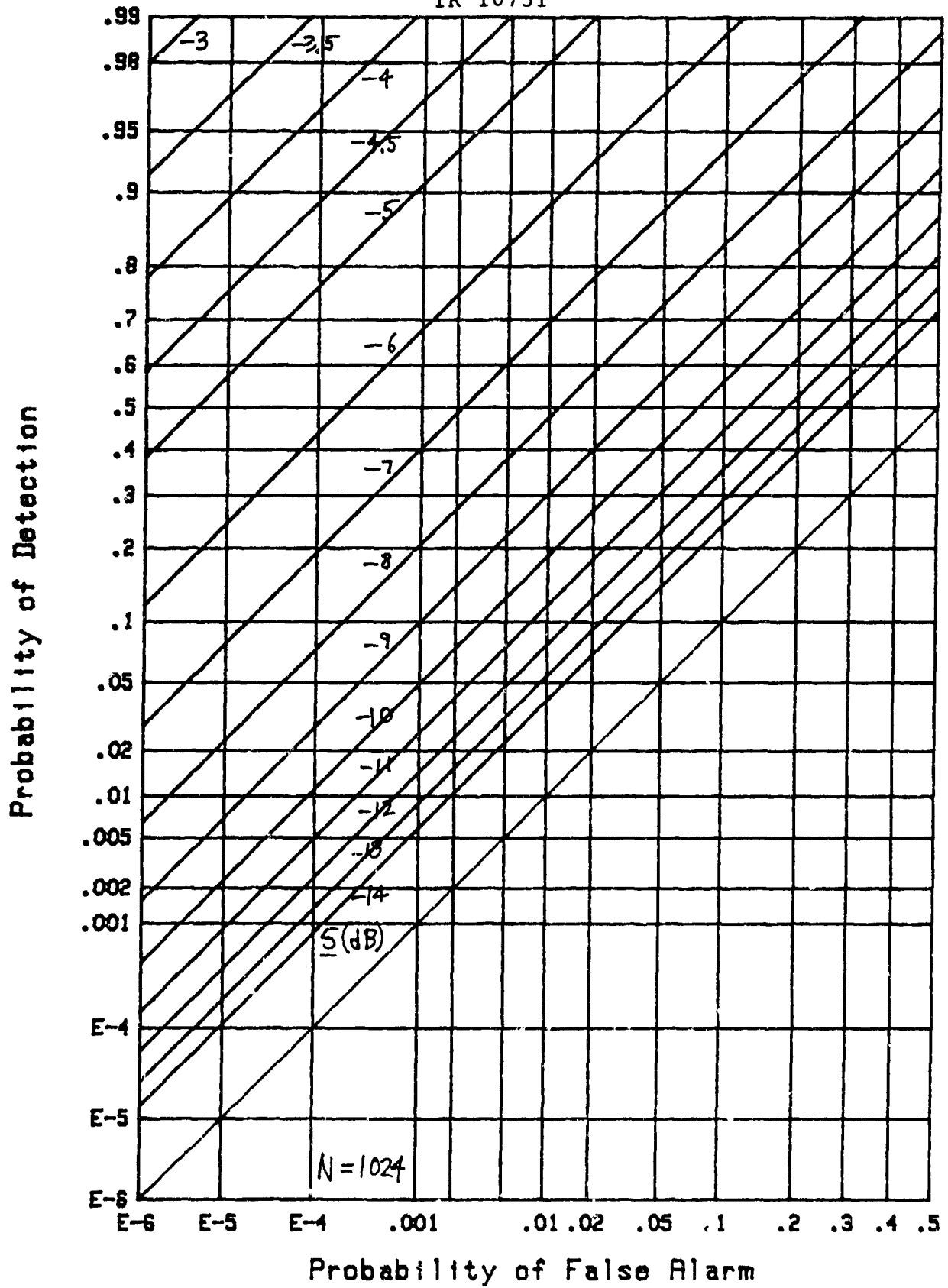
Figure A-11.   Operating Characteristic for $\nu = 2$, $\underline{M} = 512$
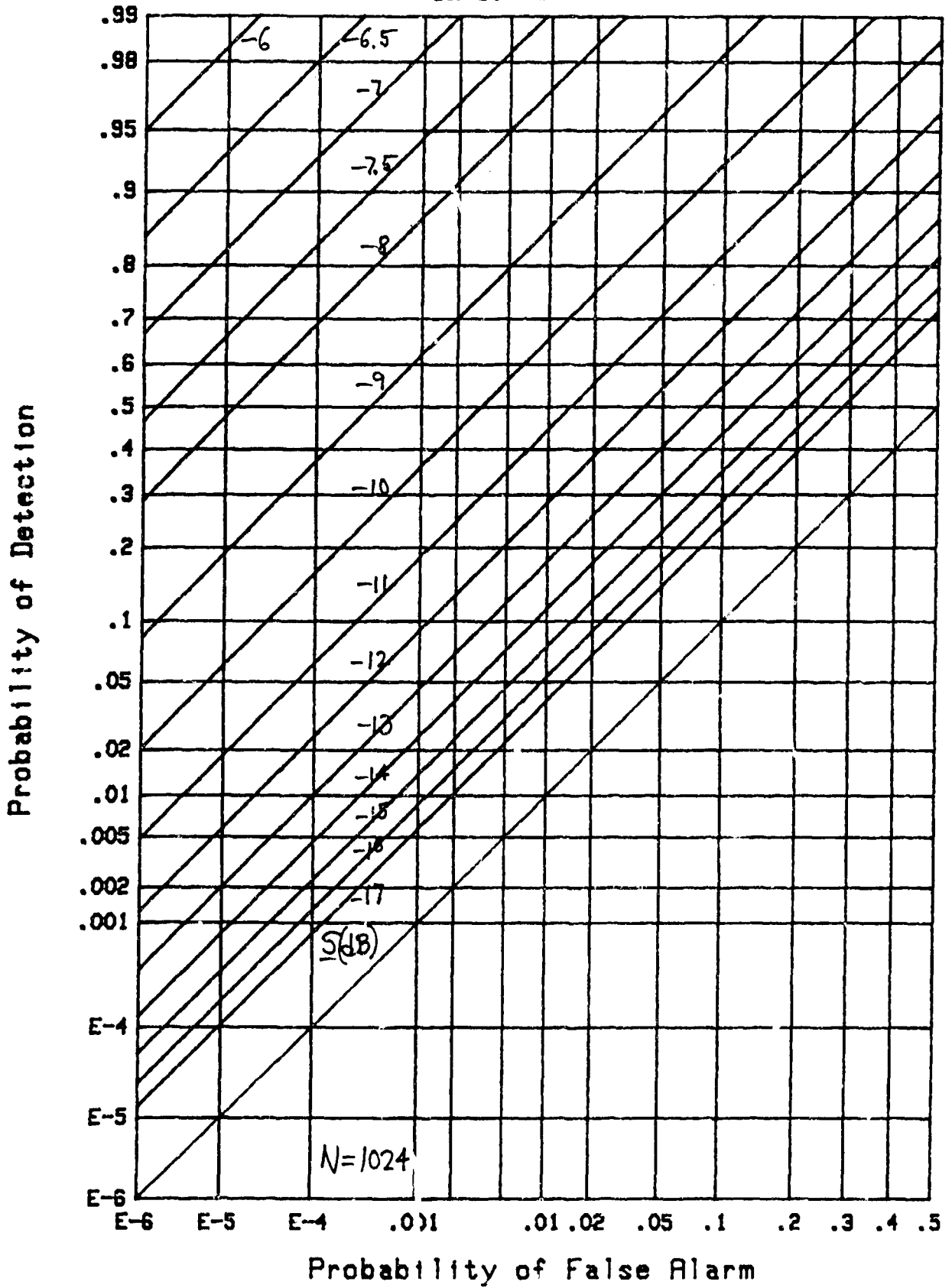
Figure A-12.   Operating Characteristic for $\nu = 2$, $\underline{M} = 1024$

APPENDIX B. RECEIVER OPERATING CHARACTERISTICS FOR $\nu = 3$

The decision variable z for this case is given by (29) as

$$z \equiv T_3 = \sum_{n=1}^{N} x_n^3 \underset{<}{>} v \; . \tag{B-1}$$

The characteristic functions of z under hypothesis H_0 is given by (24), in conjunction with (30) for $\underline{a} = 1$. The exceedance distribution function of z under hypothesis H_1 was determined by simulation with at least 10,000 independent trials; this yields the curves of P_d versus threshold v. Ten different values of average signal power per bin, $\underline{S}$, were run. Also, twelve values of $\underline{M}$, the number of bins occupied by signal, have been considered; they are

$$\underline{M} = 1, \; 2, \; 3, \; 4, \; 8, \; 16, \; 32, \; 64, \; 128, \; 256, \; 512, \; 1024, \tag{B-2}$$

and the corresponding receiver operating characteristics are plotted in figures B-1 through B-12, respectively. The curves are labeled by the parameter $\underline{S}$(dB), which is equal to $10 \log_{10}(\underline{S})$. Thus, $\underline{S}$(dB) can be interpreted as the required signal-to-noise ratio per bin in decibels. The total search size, N, is kept fixed at value 1024 for all these plots.
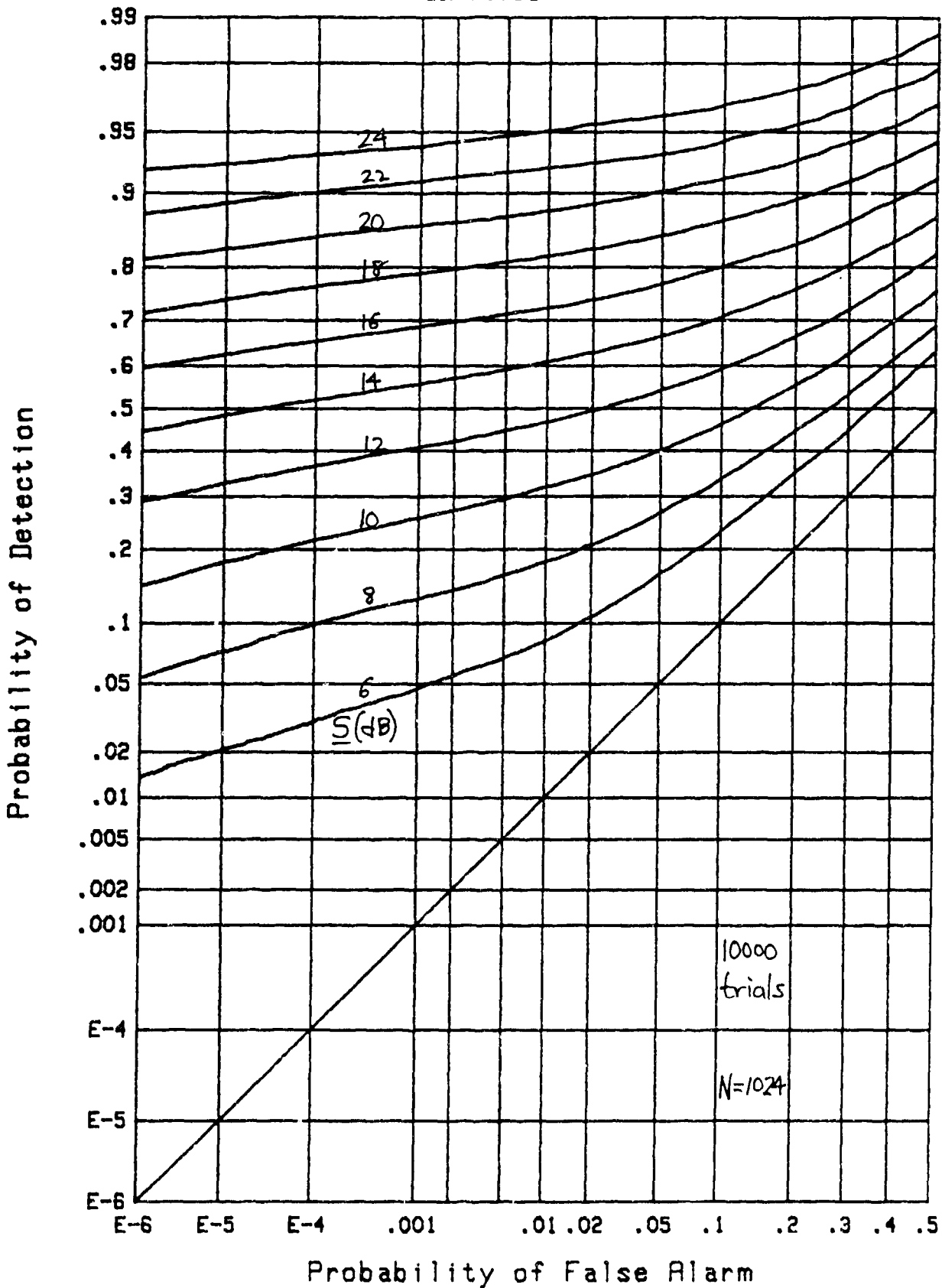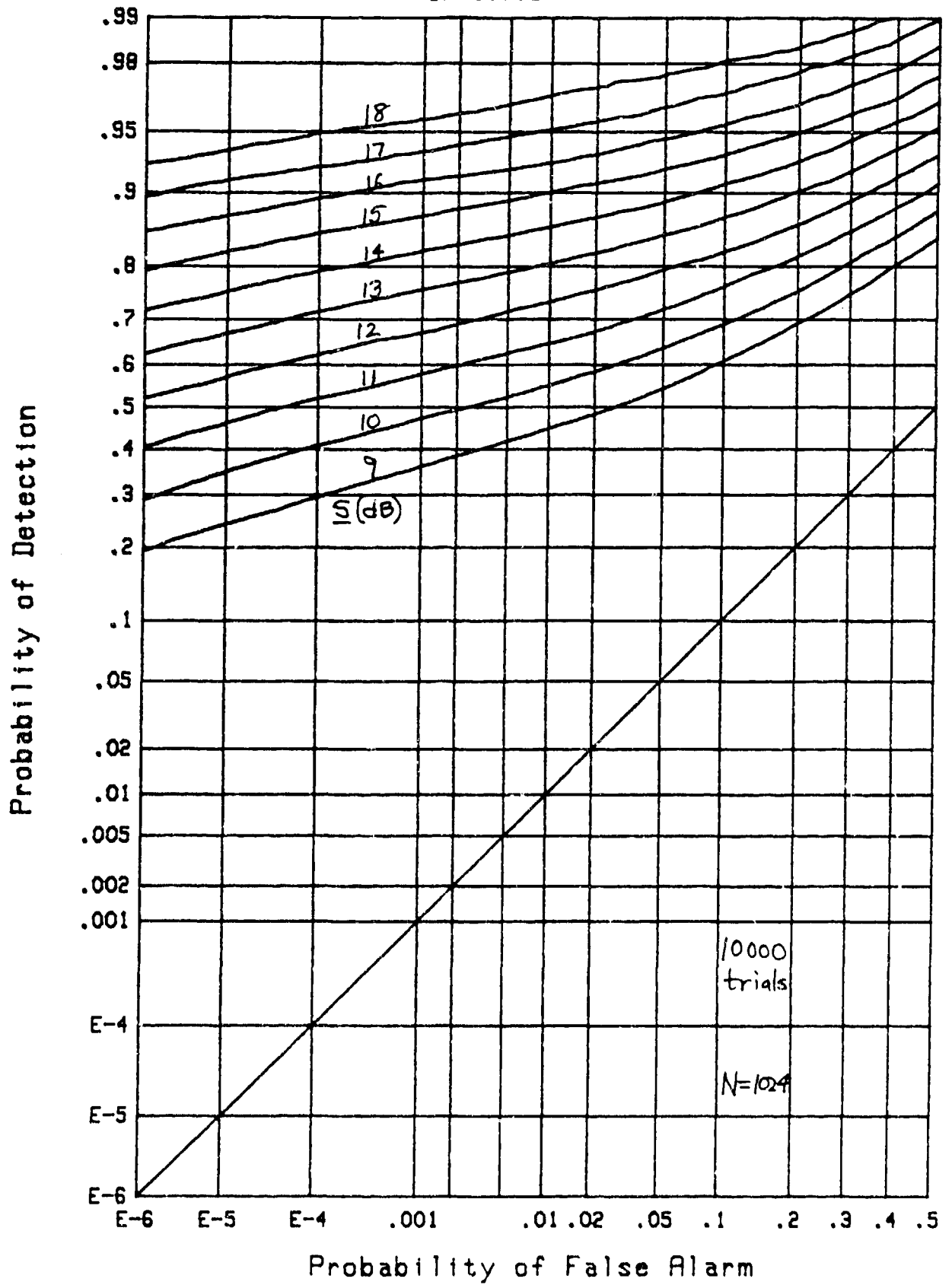
Figure B-1.   Operating Characteristic for $\nu = 3$, $\underline{M} = 1$
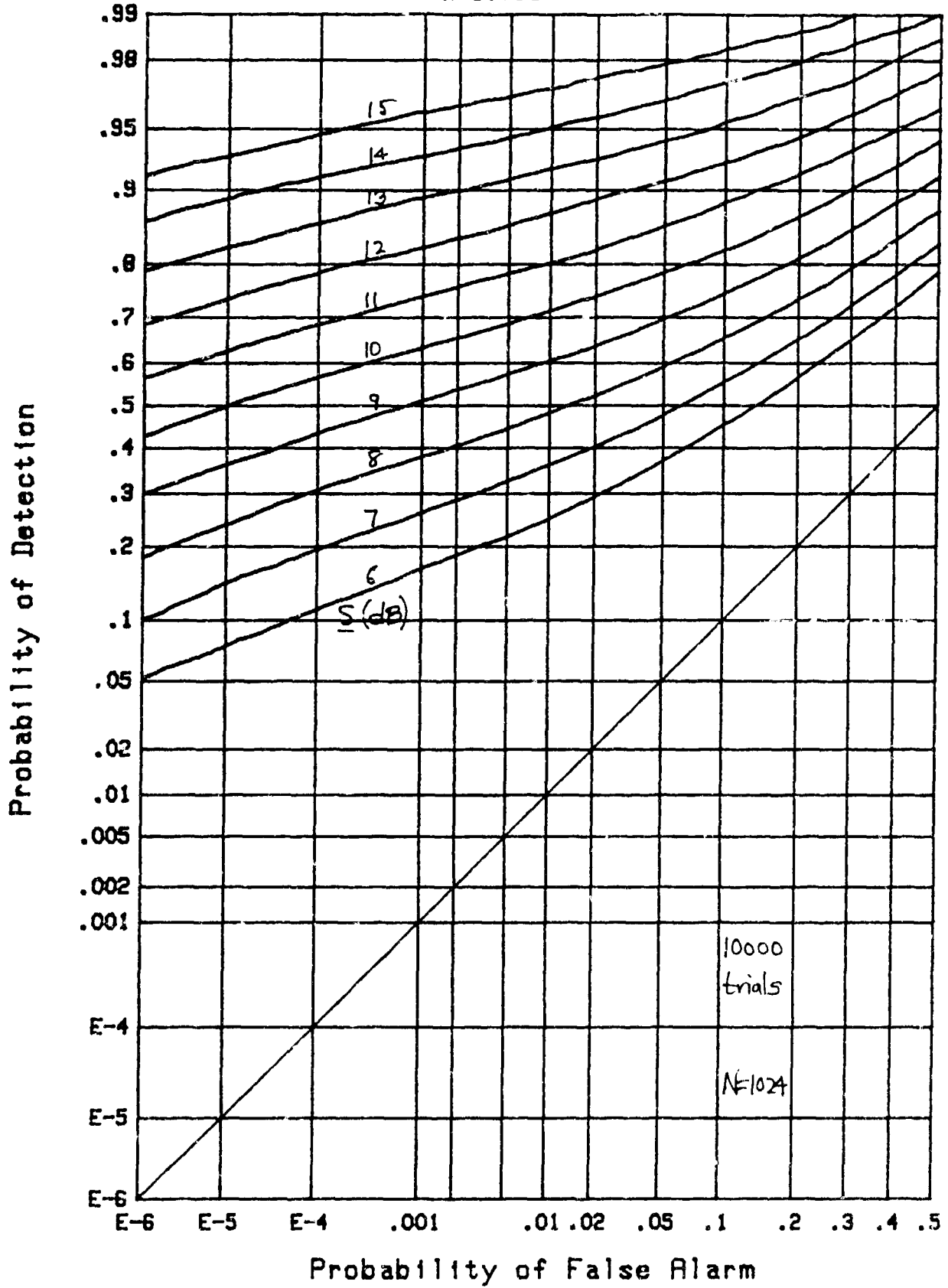
Figure B-2. Operating Characteristic for $\nu = 3$, $\underline{M} = 2$

49

Figure B-3.   Operating Characteristic for $\nu = 3$, $\underline{M} = 3$
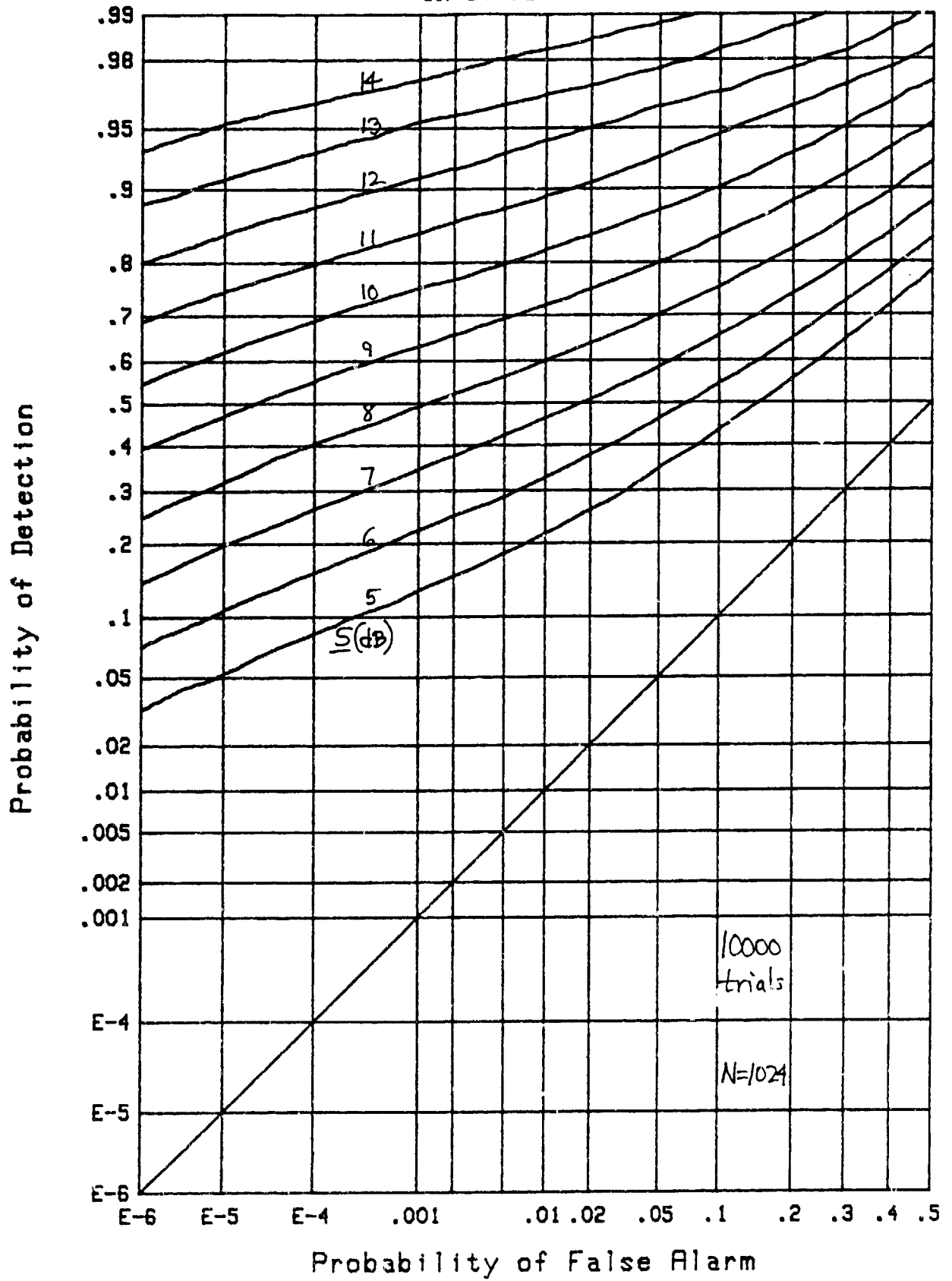
Figure B-4.   Operating Characteristic for $\nu = 3$, $\underline{M} = 4$

51
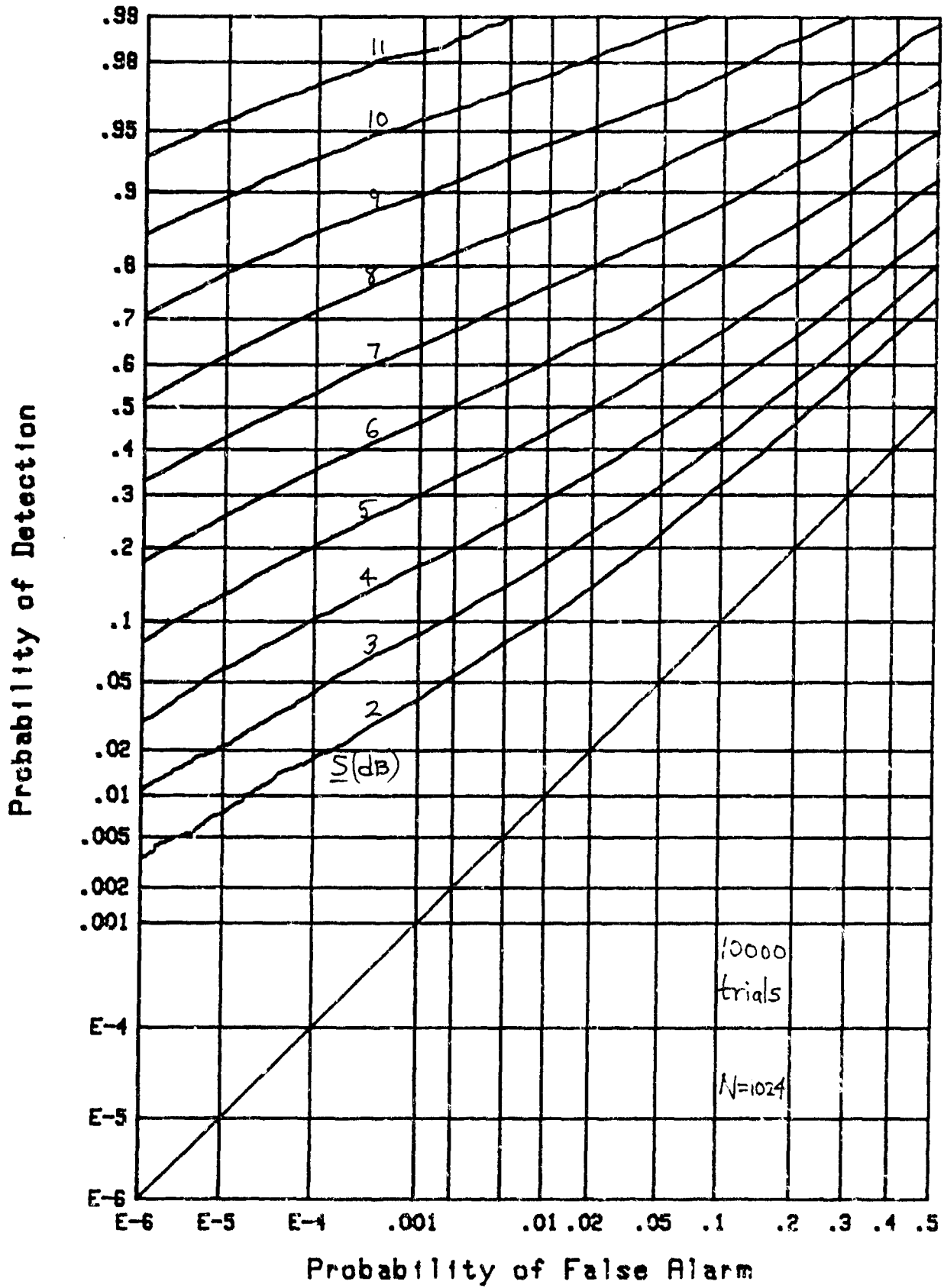
Figure B-5.   Operating Characteristic for $\nu = 3$, $\underline{M} = 8$
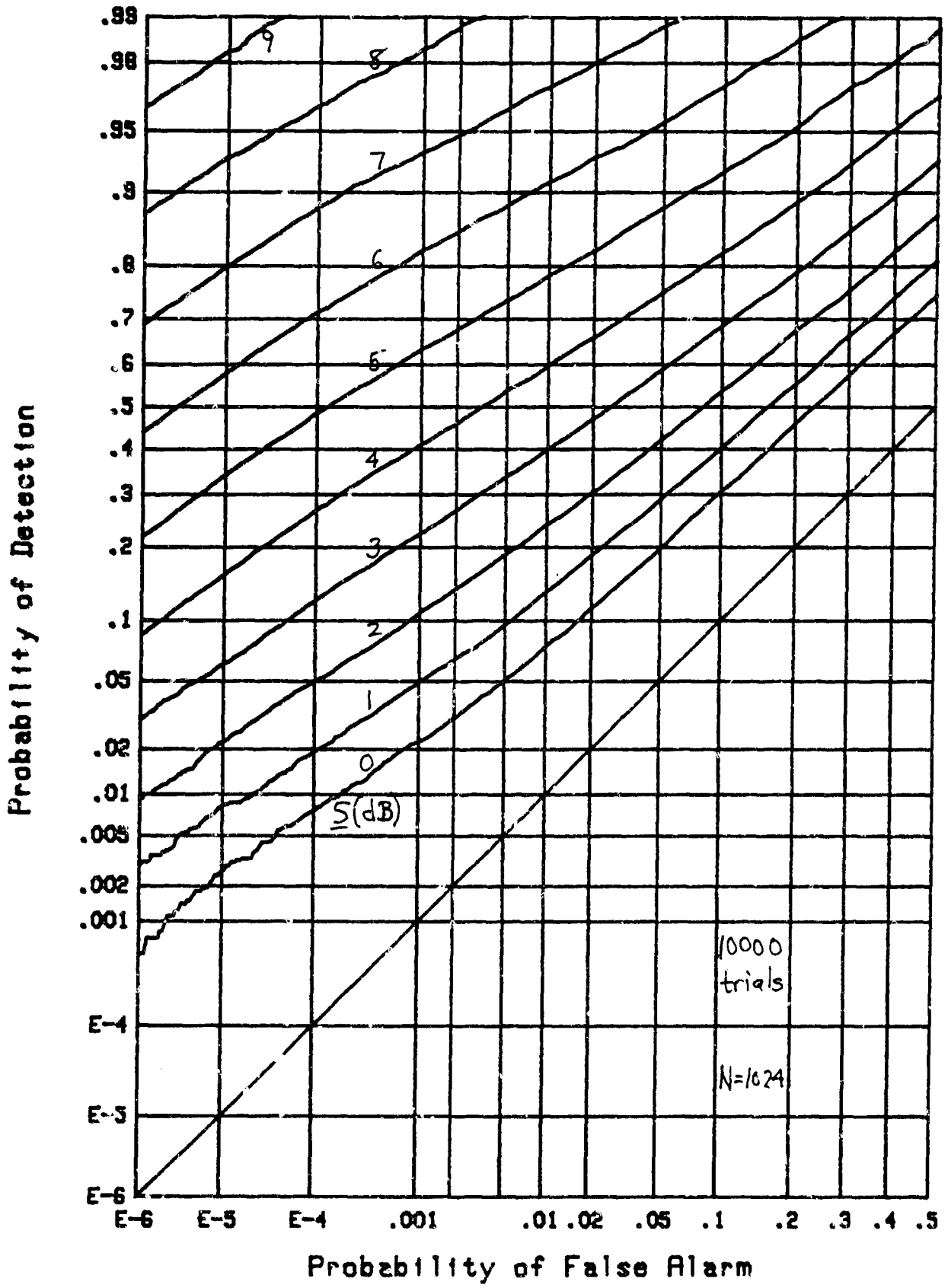
Figure B-6. Operating Characteristic for $\nu = 3$, $\underline{M} = 16$
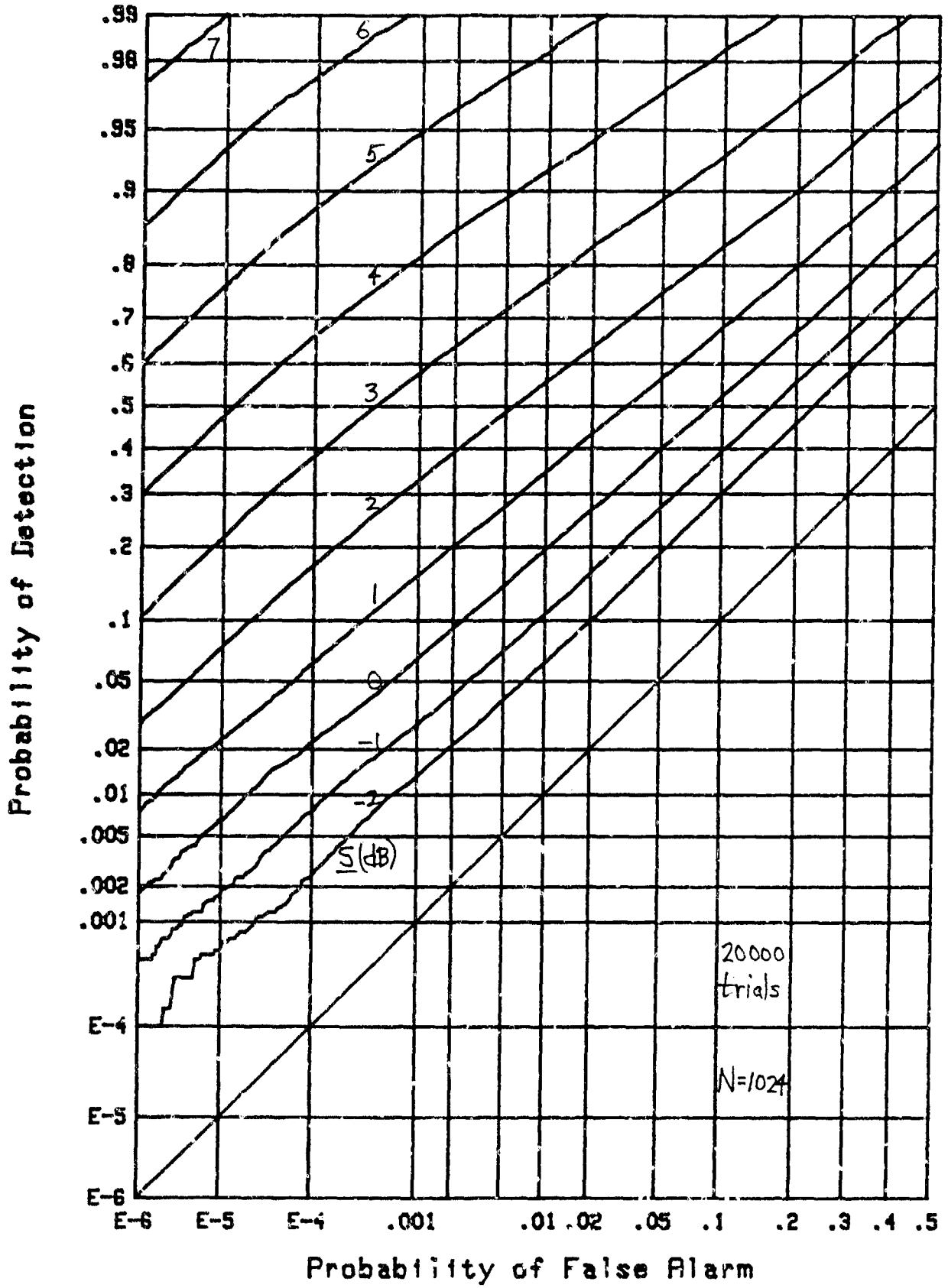
Figure B-7. Operating Characteristic for $\nu = 3$, $\underline{M} = 32$
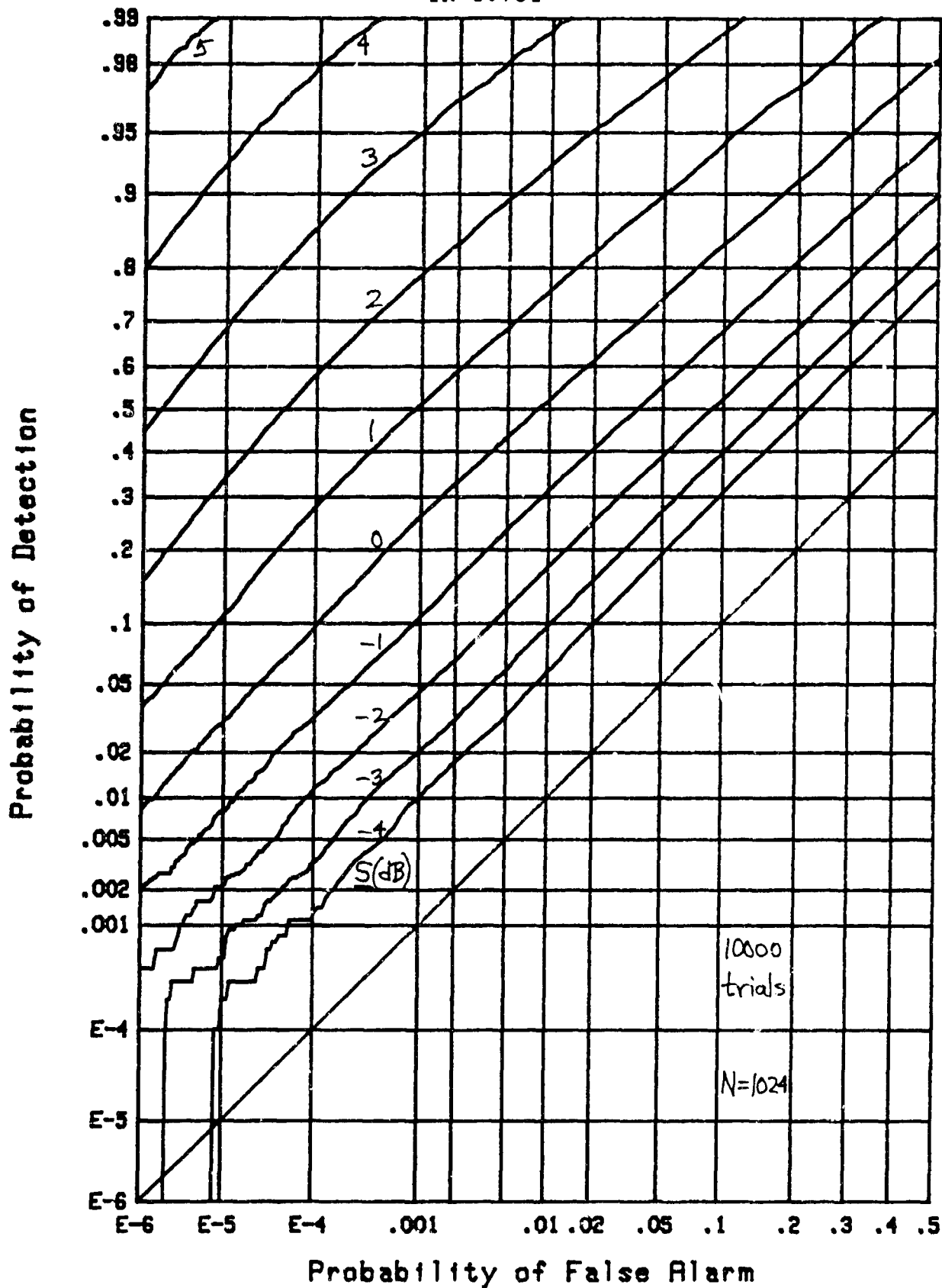
Figure B-8. Operating Characteristic for $\nu = 3$, $\underline{M} = 64$
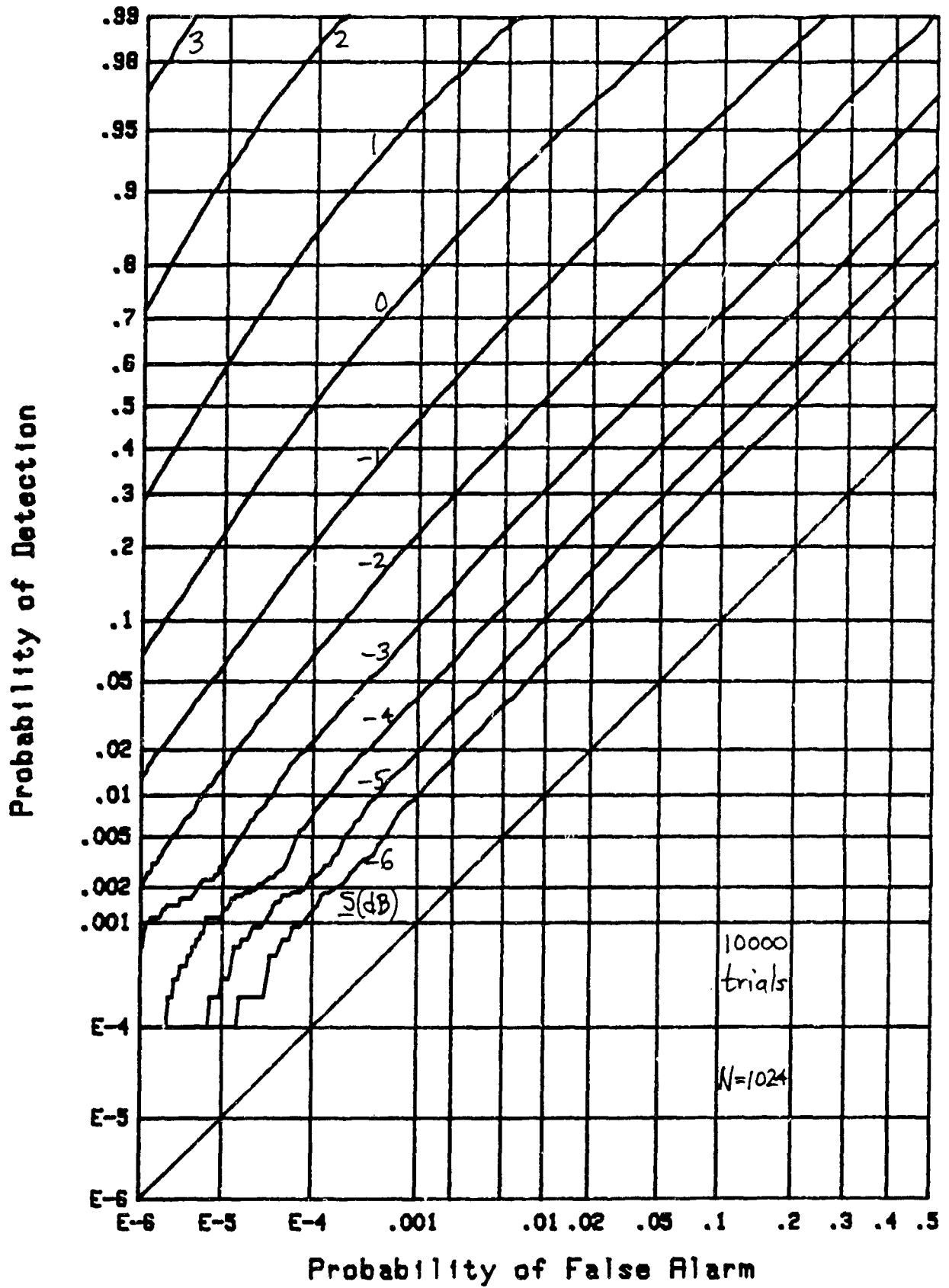
Figure B-9. Operating Characteristic for $\nu = 3$, $\underline{M} = 128$
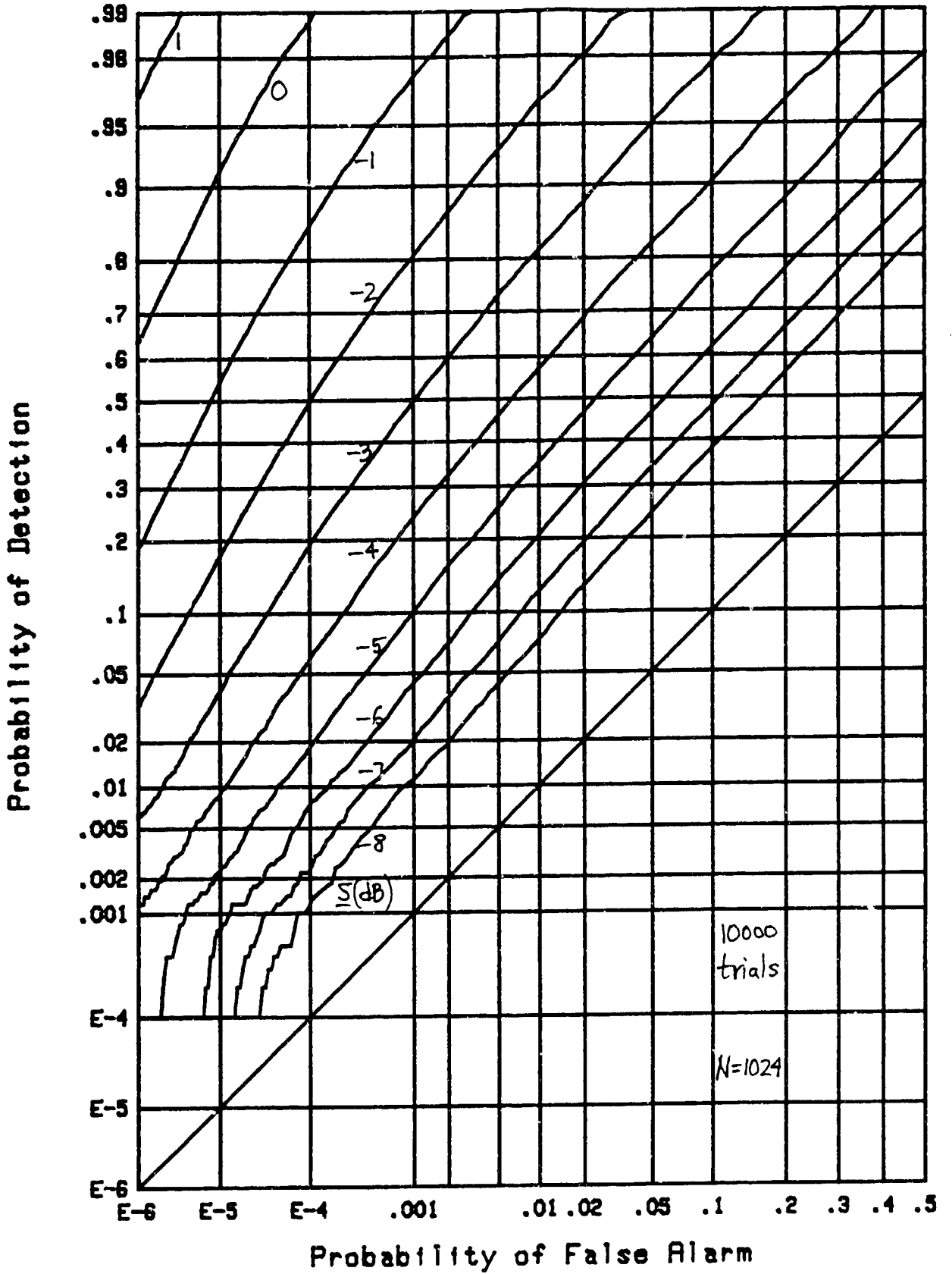
Figure B-10. Operating Characteristic for $\nu = 3$, $\underline{M} = 256$
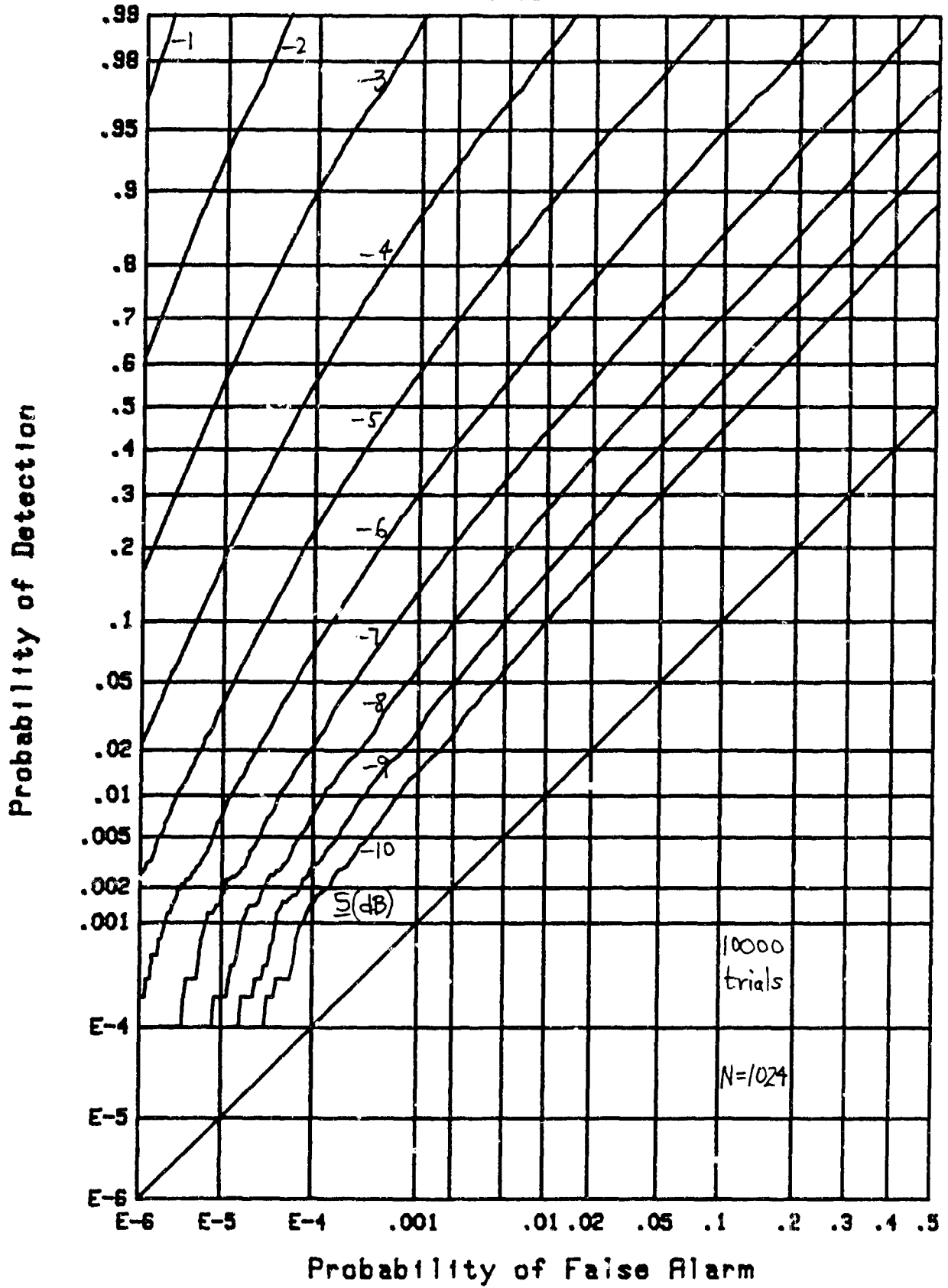
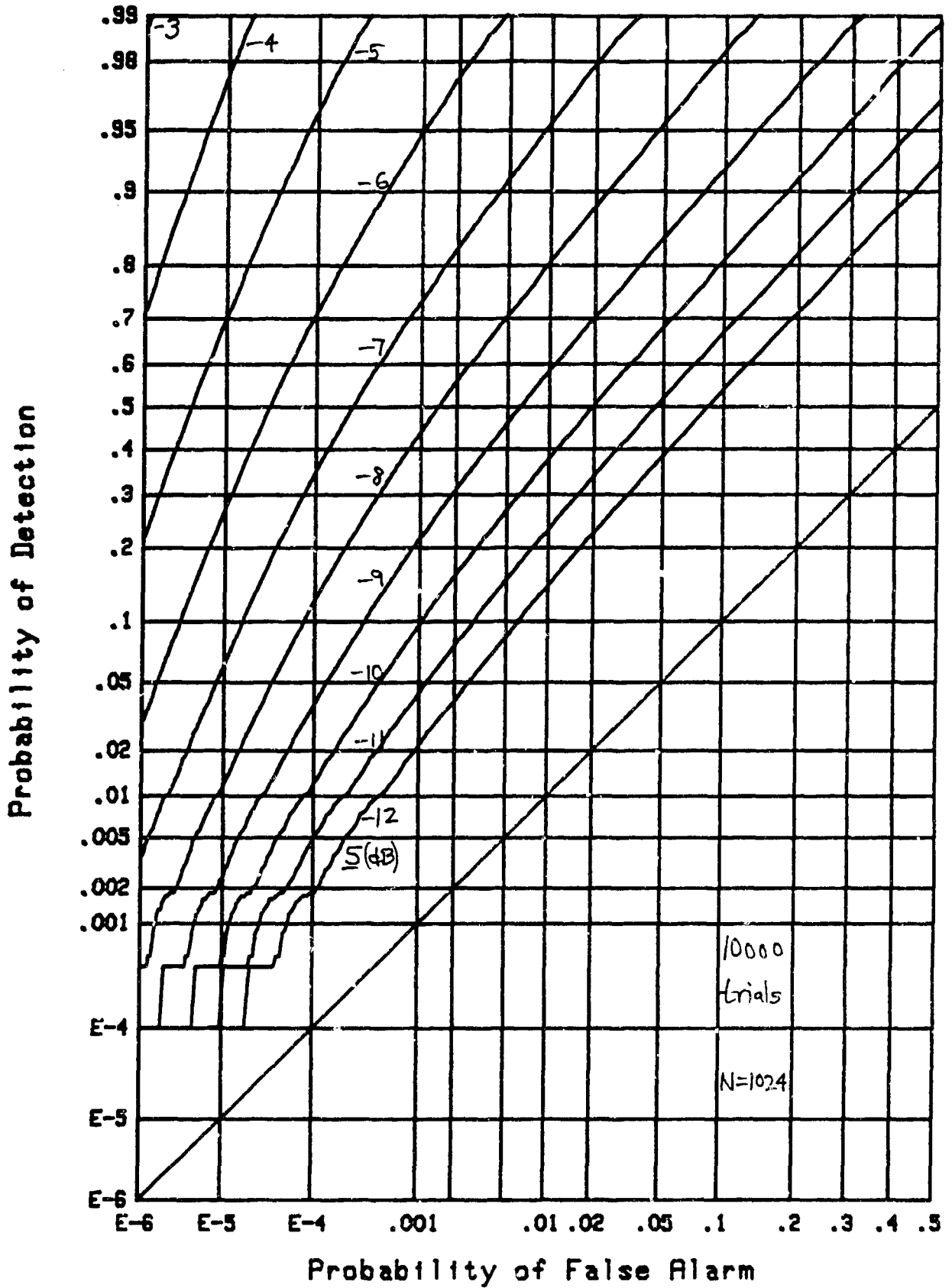Figure B-11. Operating Characteristic for $\nu = 3$, $\underline{M} = 512$

Figure B-12.   Operating Characteristic for $\nu = 3$, $\underline{M} = 1024$

APPENDIX C.   RECEIVER OPERATING CHARACTERISTICS FOR $\nu = 2.5$

The decision variable z for this case is given by (31) as

$$z \equiv T_\nu = \sum_{n=1}^{N} x_n^\nu \underset{<}{\overset{>}{}} v , \qquad (C-1)$$

where we now take power $\nu = 2.5$. The characteristic functions of z under hypothesis H_0 is given by (24), in conjunction with (32). The exceedance distribution function of z under hypothesis H_1 was determined by simulation with at least 10,000 independent trials; this yields the curves of P_d versus threshold v. Ten different values of average signal power per bin, $\underline{S}$, were run. Also, twelve values of $\underline{M}$, the number of bins occupied by signal, have been considered; they are

$$\underline{M} = 1, 2, 3, 4, 8, 16, 32, 64, 128, 256, 512, 1024, \qquad (C-2)$$

and the corresponding receiver operating characteristics are plotted in figures C-1 through C-12, respectively. The curves are labeled by the parameter $\underline{S}(dB)$, which is equal to $10 \log_{10}(\underline{S})$. Thus, $\underline{S}(dB)$ can be interpreted as the required signal-to-noise ratio per bin in decibels. The total search size, N, is kept fixed at value 1024 for all these plots.
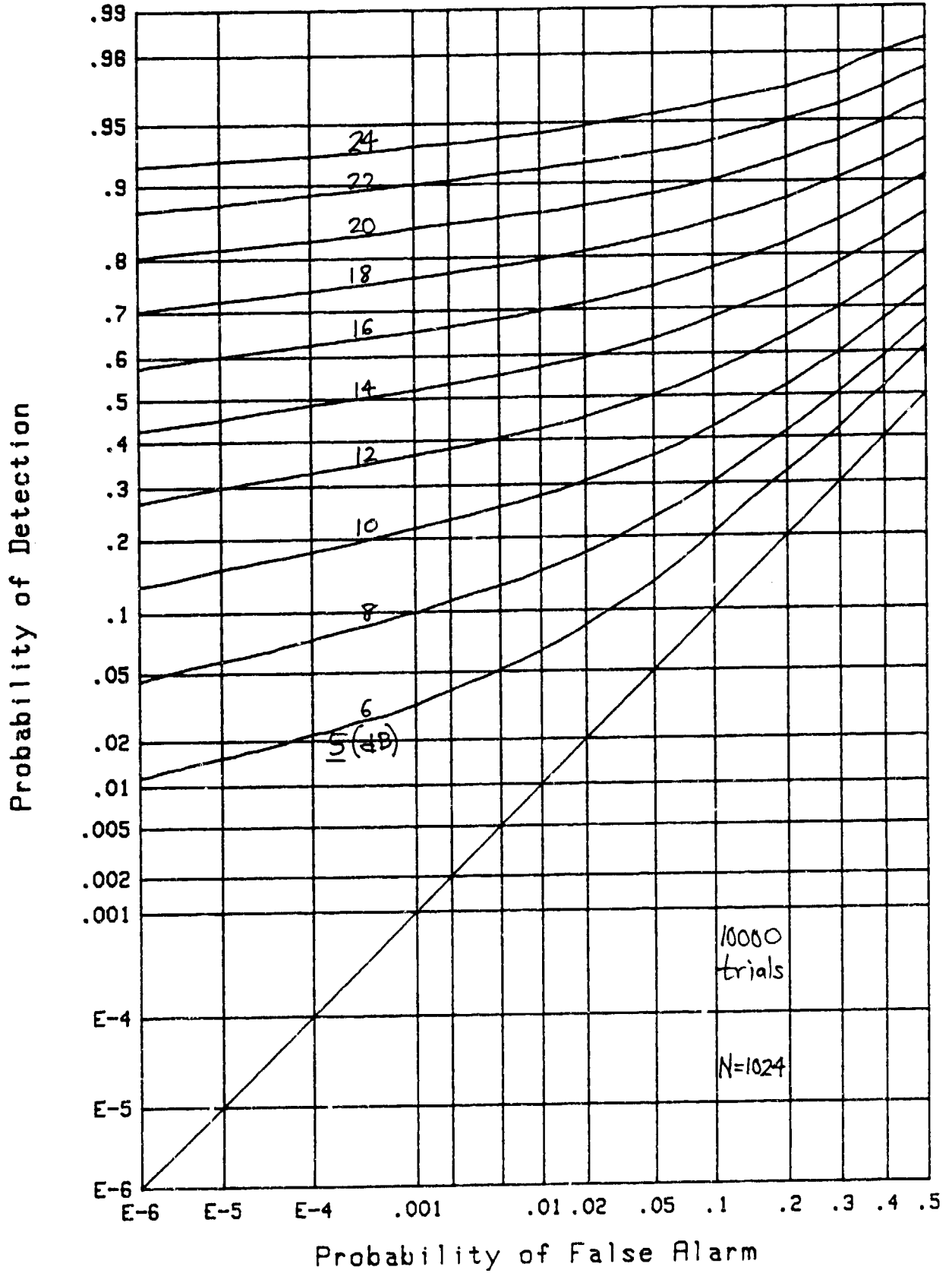
Figure C-1.   Operating Characteristic for ν = 2.5, $\underline{M}$ = 1
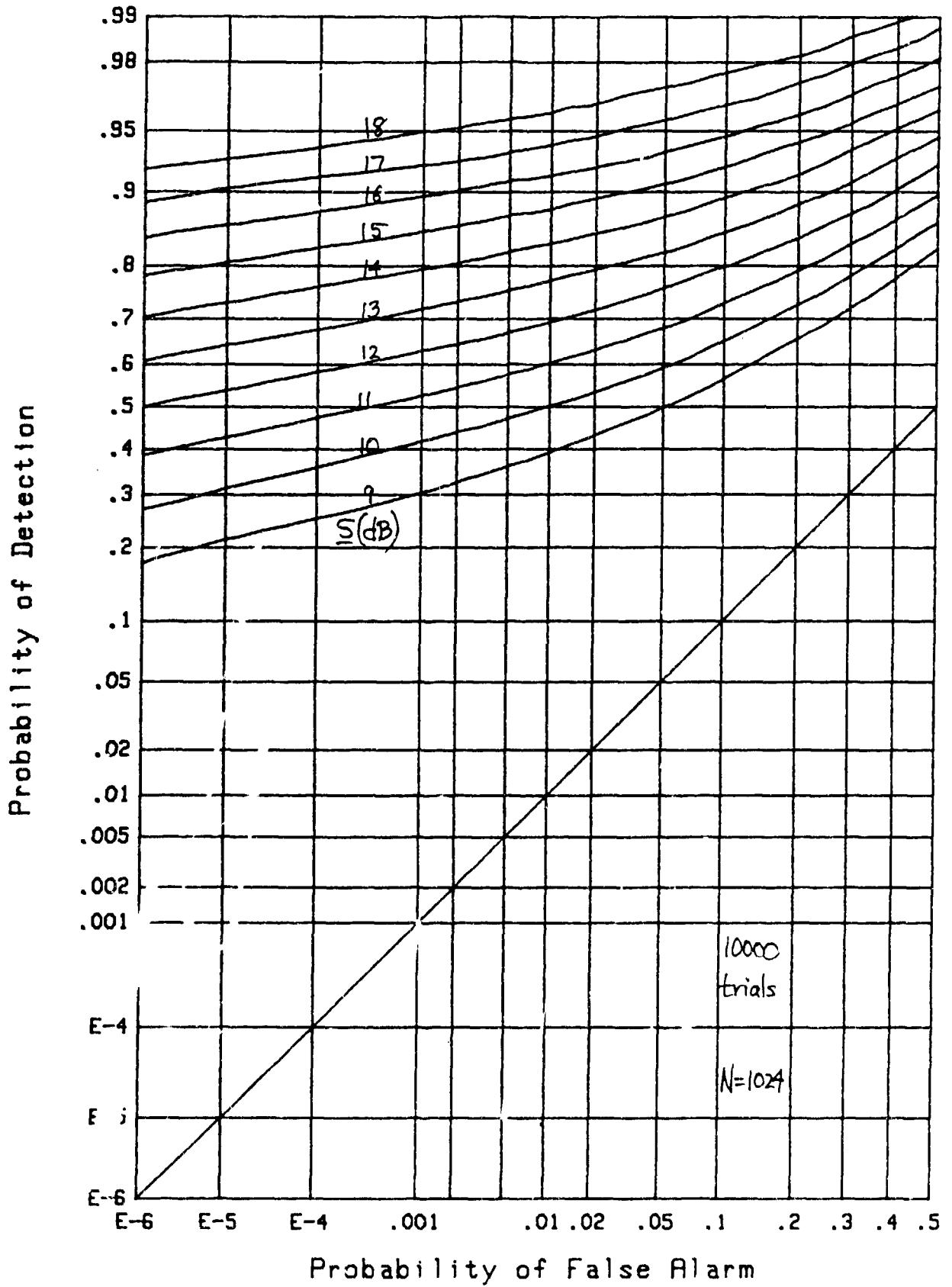
Figure C-2. Operating Characteristic for $v = 2.5$, $\underline{M} = 2$
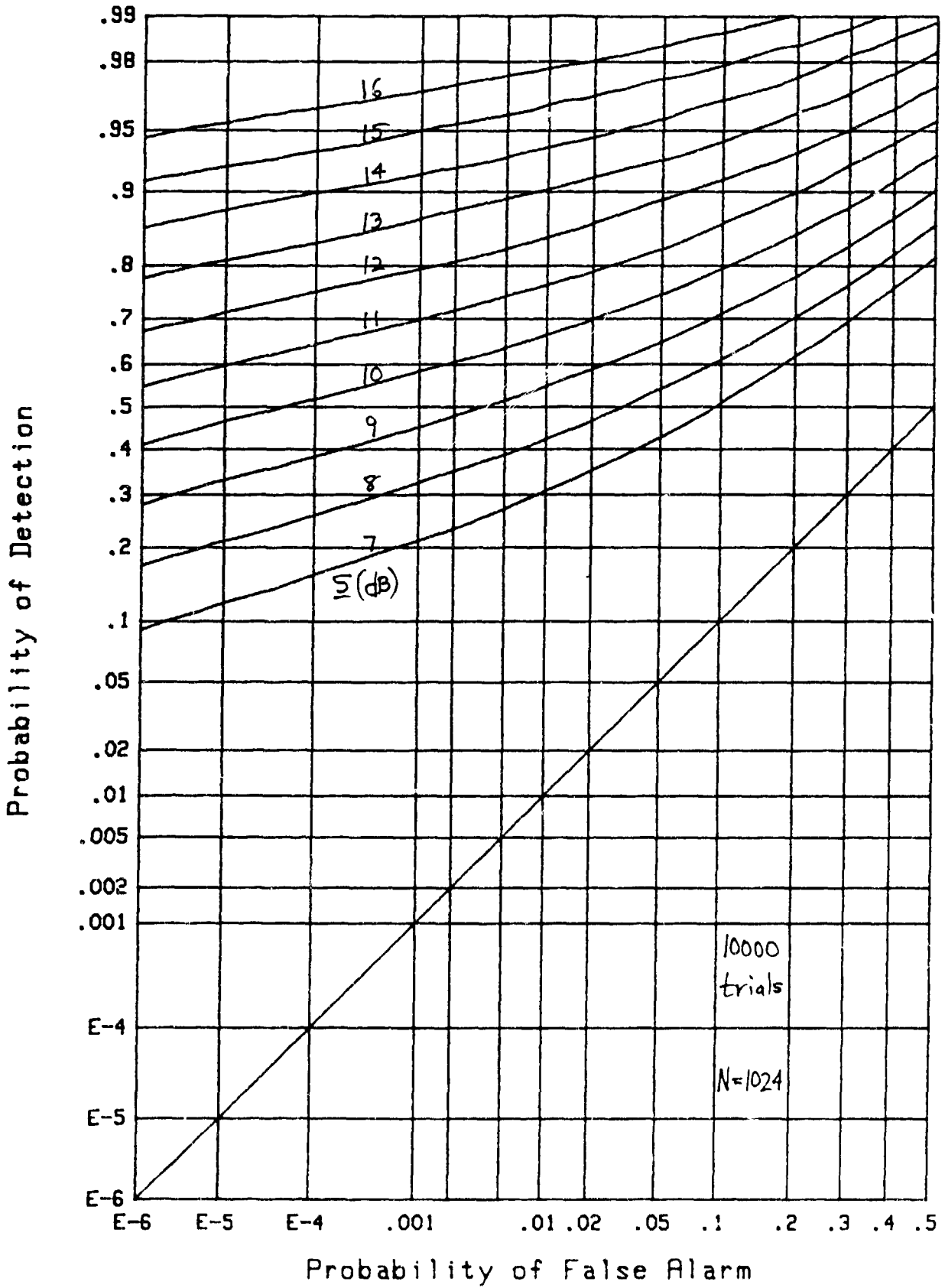
Figure C-3.   Operating Characteristic for $\nu = 2.5$, $\underline{M} = 3$
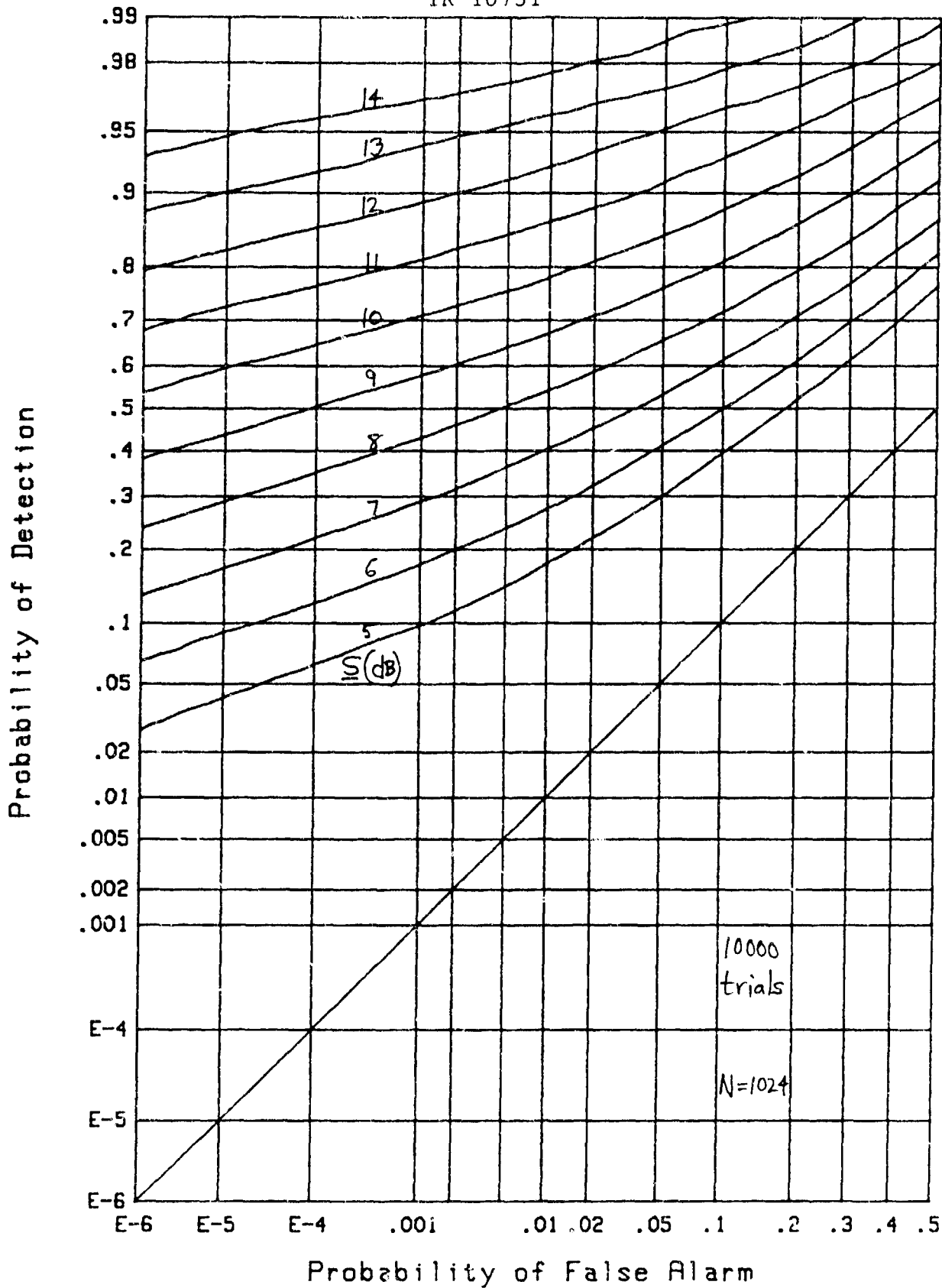
Figure C-4. Operating Characteristic for $\nu = 2.5$, $\underline{M} = 4$
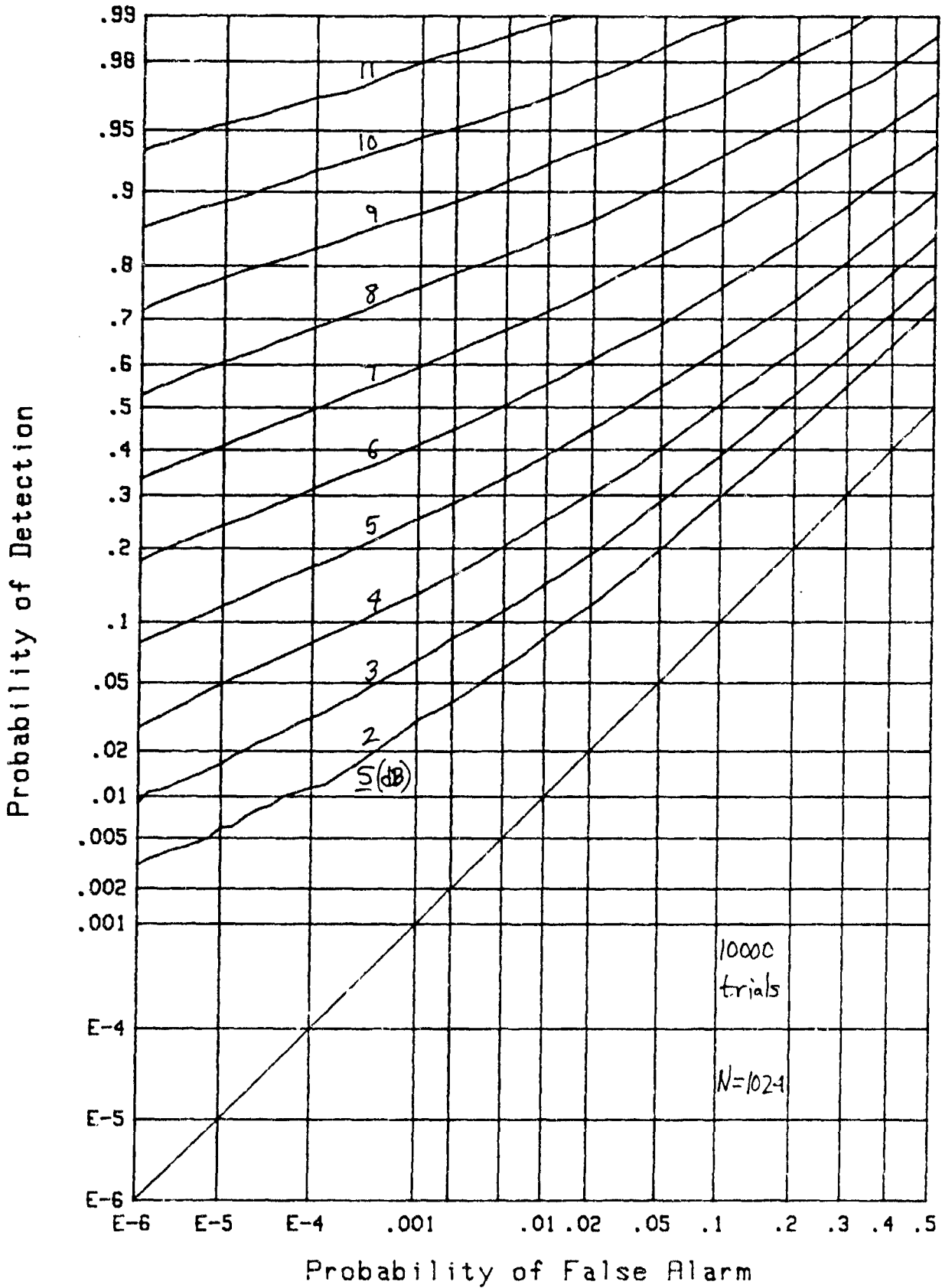
Figure C-5. Operating Characteristic for $\nu = 2.5$, $\underline{M} = 8$
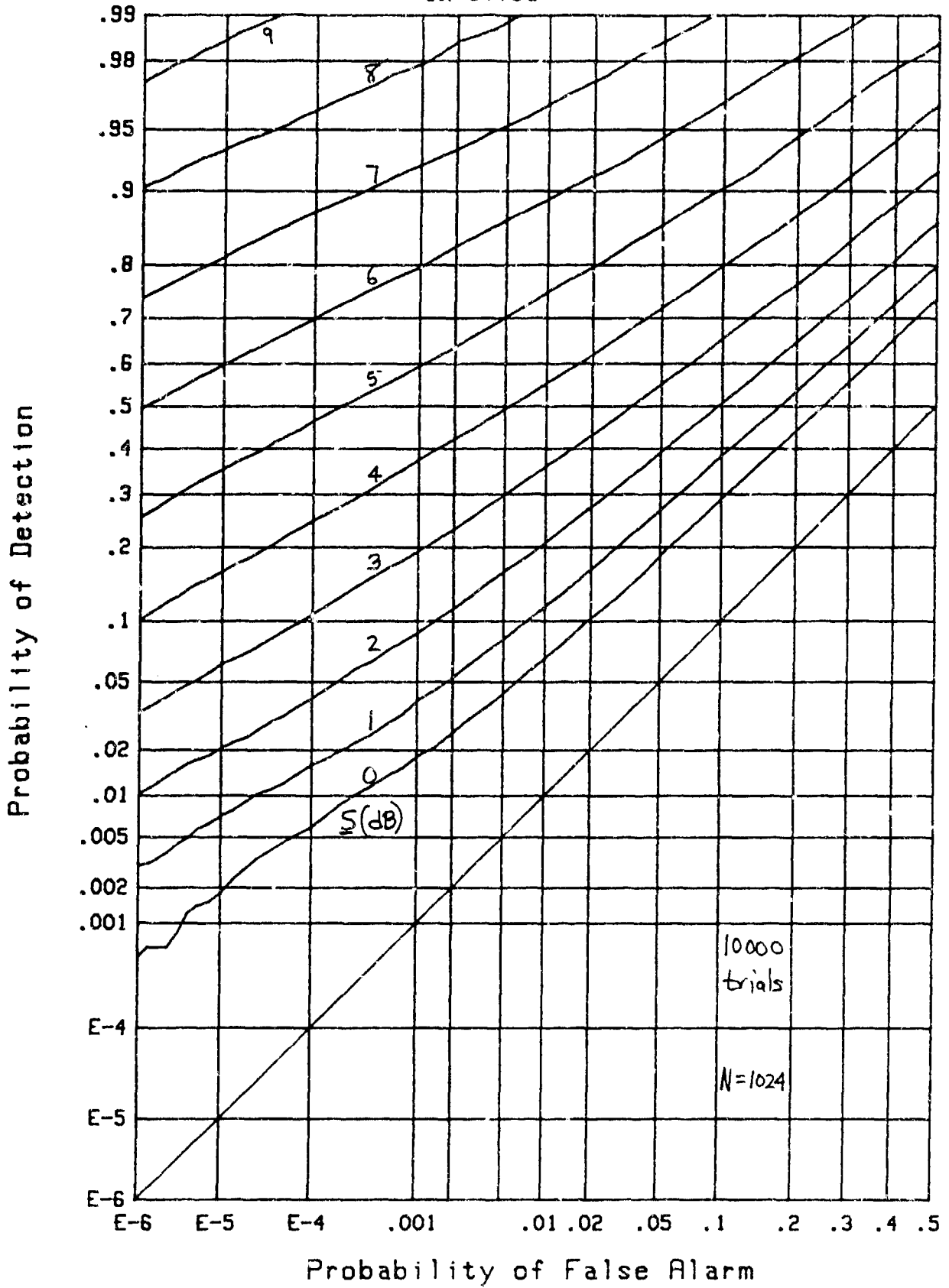
Figure C-6. Operating Characteristic for $\nu = 2.5$, $\underline{M} = 16$
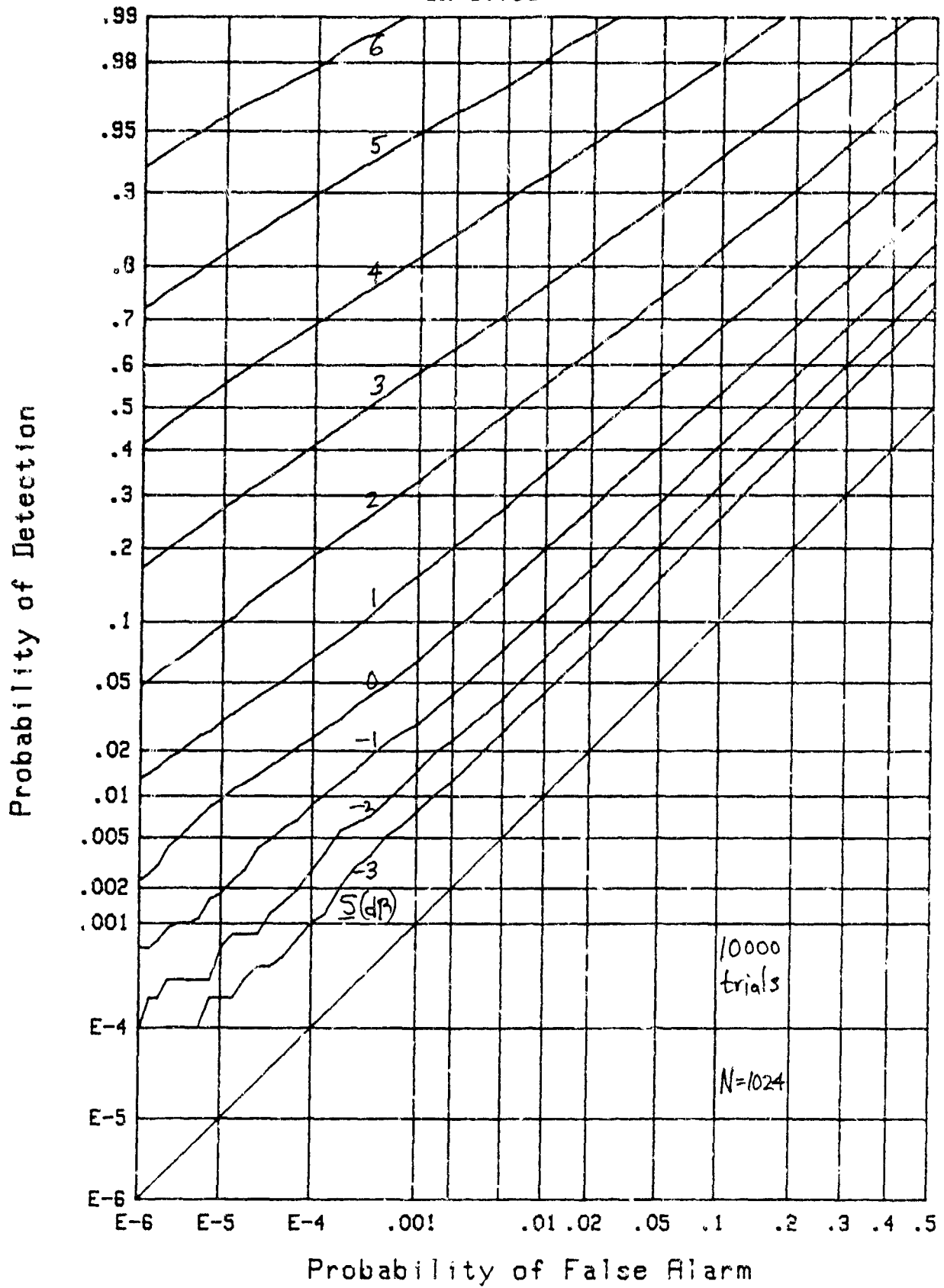
Figure C-7.   Operating Characteristic for $\nu = 2.5$, $\underline{M} = 32$
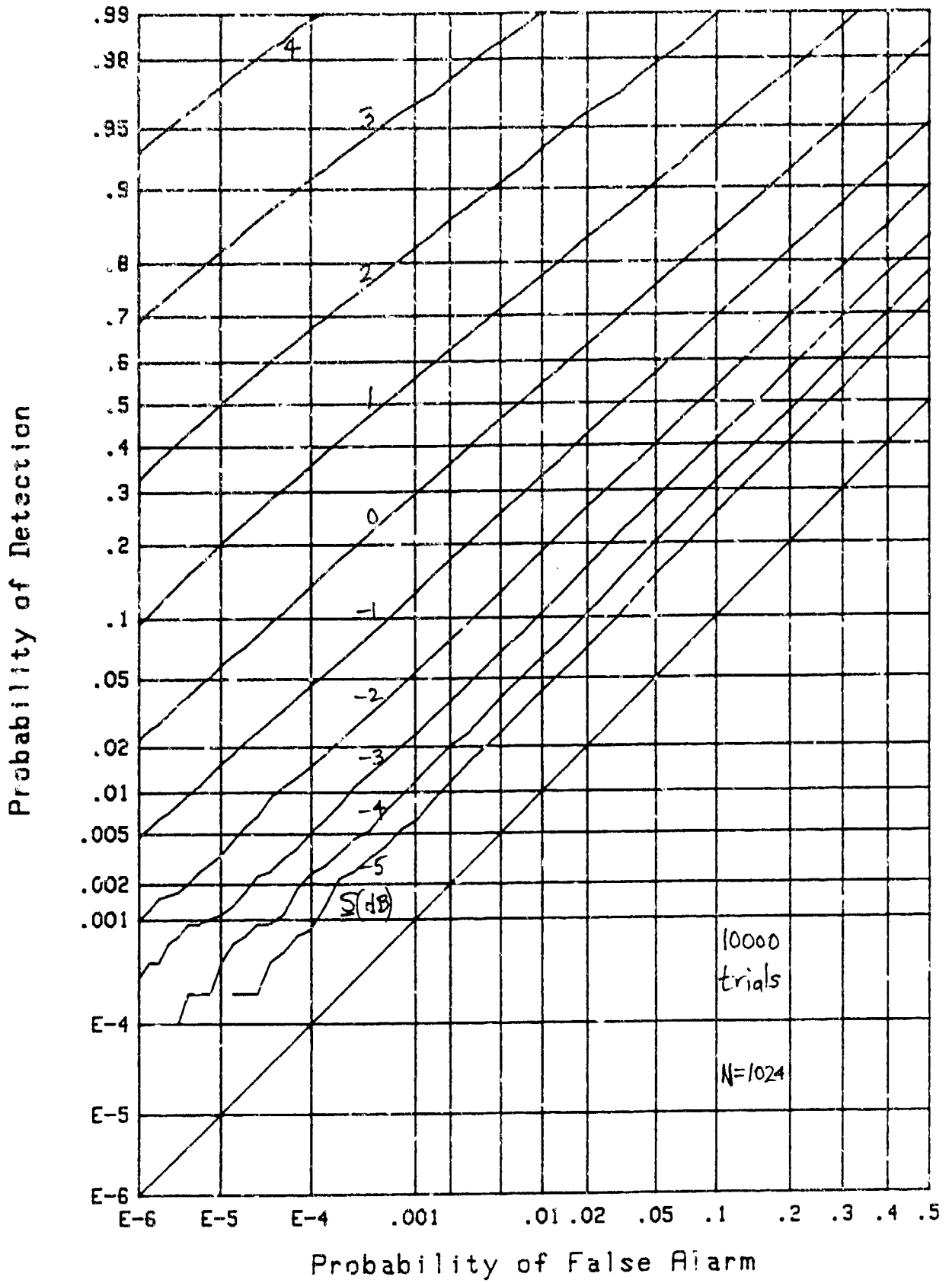
Figure C-8. Operating Characteristic for $\nu = 2.5$, $\underline{M} = 64$
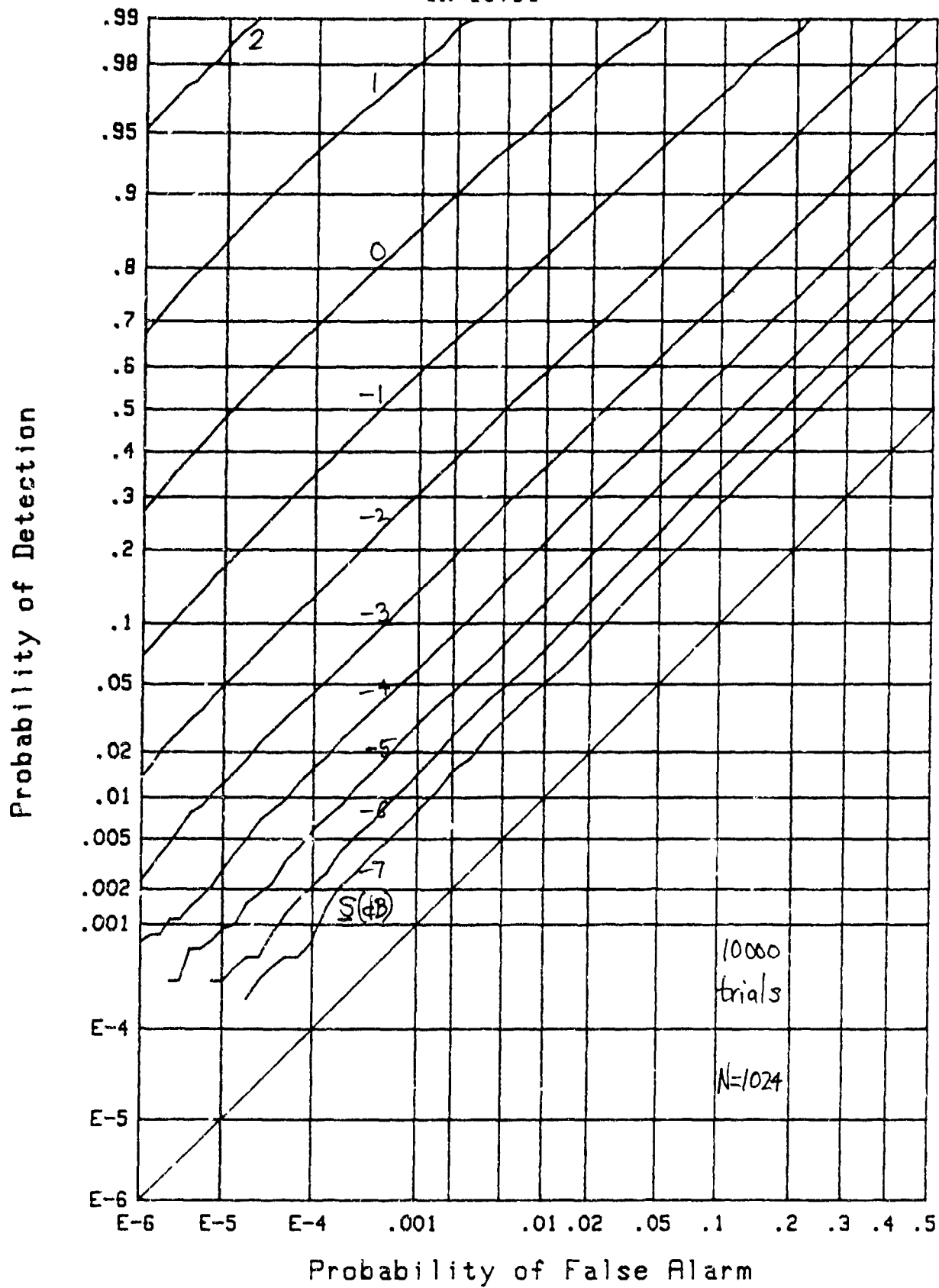
Figure C-9. Operating Characteristic for $\nu = 2.5$, $\underline{M} = 128$
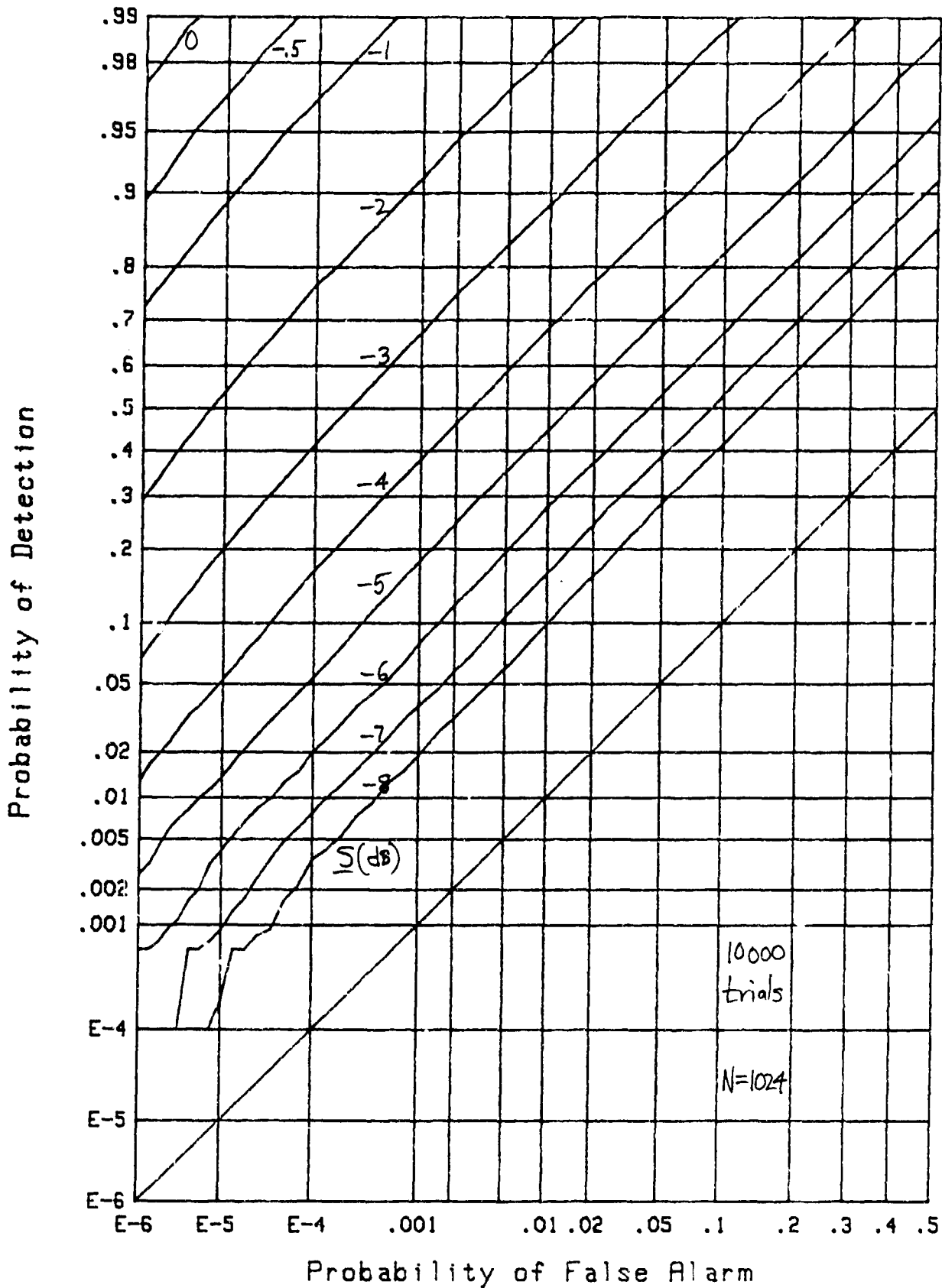
Figure C-10.   Operating Characteristic for $\nu = 2.5$, $\underline{M} = 256$
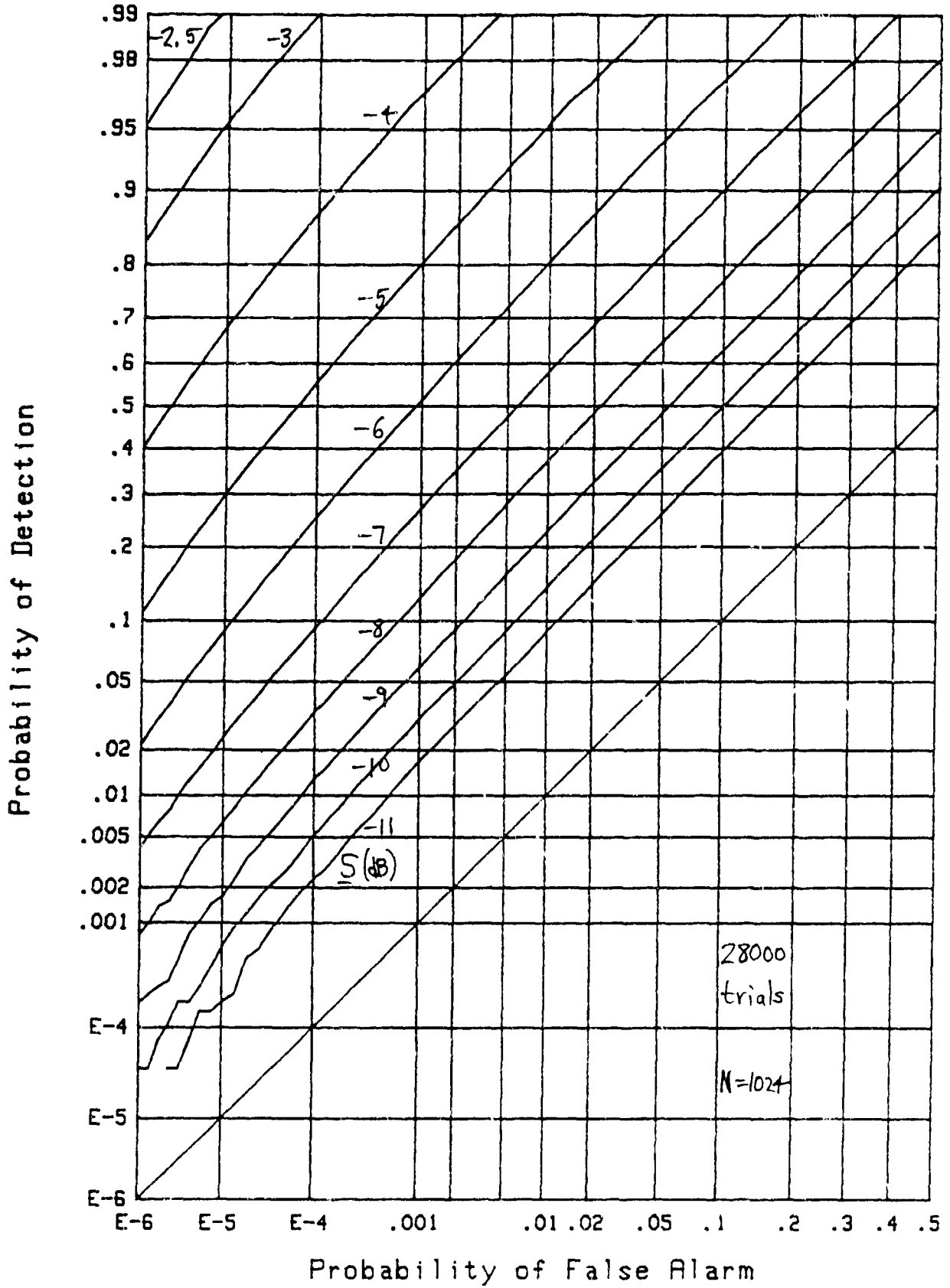
Figure C-11.   Operating Characteristic for $\nu = 2.5$, $\underline{M} = 512$
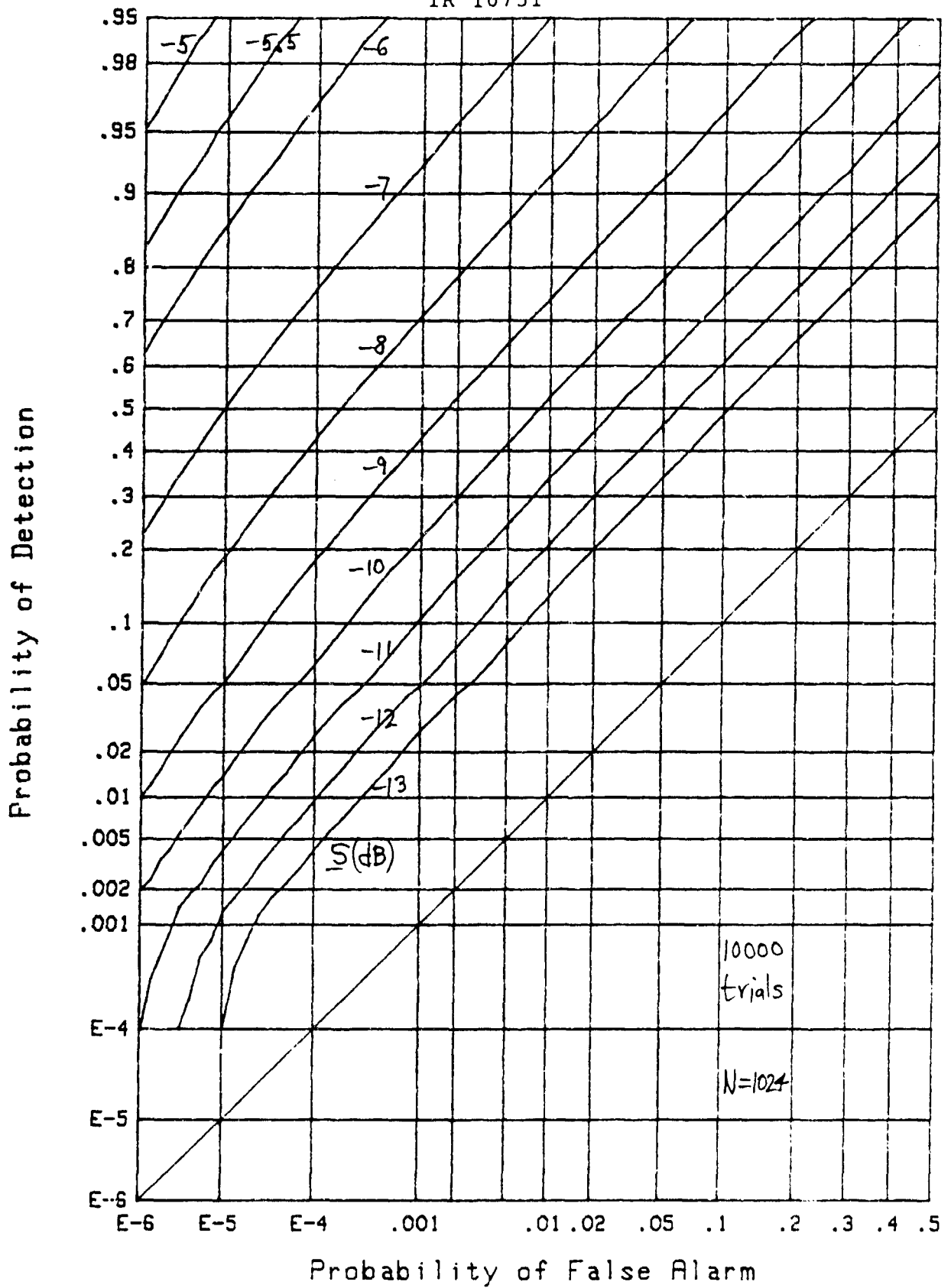
Figure C-12. Operating Characteristic for ν = 2.5, M = 1024

REFERENCES

[1]   A. H. Nuttall, Detection Performance of a Modified Generalized Likelihood Ratio Processor for Random Signals of Unknown Location, NUWC-NPT Technical Report 10539, Naval Undersea Warfare Center Detachment, New London, CT, 23 November 1993.

[2]   A. H. Nuttall, Detection Performance of Generalized Likelihood Ratio Processors for Random Signals of Unknown Location, Structure, Extent, and Strength, NUWC-NPT Technical Report 10739, Naval Undersea Warfare Center Division, Newport, RI, 25 August 1994.

[3]   B. H. Maranda and J. A. Fawcett, "The Performance Analysis of a Fourth-Moment Detector", Proceedings IEEE International Conference, Acoustics, Speech, and Signal Processing, Albuquerque, NM, pages 1357 - 1360, 3 - 6 April 1990.

[4]   J. A. Fawcett and B. H. Maranda, "The Optimal Power Law for the Detection of a Gaussian Burst in a Background of Gaussian Noise", IEEE Transactions on Information Theory, volume 37, number 1, pages 209 - 214, January 1991.

[5]   Handbook of Mathematical Functions, U. S. Department of Commerce, National Bureau of Standards, Applied Mathematics Series, number 55, U. S. Government Printing Office, Washington, DC, June 1964.

[6]   A. H. Nuttall, Accurate Efficient Evaluation of Cumulative
or Exceedance Probability Distributions Directly From
Characteristic Functions, NUSC Technical Report 7023, Naval
Underwater Systems Center, New London, CT, 1 October 1983.

[7]   A. H. Nuttall, Limiting Detection Performance for Random
Signals of Unknown Location, Structure, Extent, and Strength,
NUWC-NPT Technical Report, Naval Undersea Warfare Center
Division, Newport, RI, in preparation.

INITIAL DISTRIBUTION LIST

Addressee	Number of Copies
Center for Naval Analyses, VA	1
Coast Guard Academy, CT	
J. Wolcin	1
Defense Technical Information Center, VA	12
Griffiss Air Force Base, NY	
Documents Library	1
J. Michels	1
National Radio Astronomy Observatory, VA	
F. Schwab	1
National Security Agency, MD	
J. Maar	1
National Technical Information Service, VA	10
Naval Air Warfare Center, PA	
Commander	1
L. Allen	1
Naval Command Control and Ocean Surveillance Center, CA	
Commanding Officer	1
J. Alsup	1
D. Hanna	1
W. Marsh	1
P. Nachtigall	1
C. Persons	1
C. Tran	1
Naval Environmental Prediction Research Facility, CA	1
Naval Intelligence Command, DC	1
Naval Oceanographic and Atmospheric Research Laboratory, CA	
M. Pastore	1
Naval Oceanographic and Atmospheric Research Laboratory, MS	
Commanding Officer	1
B. Adams	1
R. Fiddler	1
E. Franchi	1
R. Wagstaff	1
Naval Oceanographic Office, MS	1
Naval Personnel Research and Development Center, CA	1
Naval Postgraduate School, CA	
Superintendent	1
C. Therrien	1
Naval Research Laboratory, DC	
Commanding Officer	1
W. Gabriel	1
A. Gerlach	1
D. Steiger	1
E. Wald	1
N. Yen	1

INITIAL DISTRIBUTION LIST (CONT'D)

Addressee	Number of Copies
Naval Research Laboratory, FL	
Superintendent	
P. Ainsleigh	1
Naval Sea Systems Command, DC	
SEA-00; -63; -63D; -63X; -92R; PMS-402	6
Naval Surface Warfare Center, FL	
Commanding Officer	1
E. Linsenmeyer	1
D. Skinner	1
Naval Surface Warfare Center, MD	
P. Prendergast	1
Naval Surface Warfare Center, VA	
J. Gray	1
Naval Surface Weapons Center, FL	1
Naval Surface Weapons Center, MD	
Officer in Charge	1
M. Strippling	1
Naval Surface Weapons Center, VA	
Commander	1
H. Crisp	1
D. Phillips	1
T. Ryczek	1
Naval Technical Intelligence Center, DC	
Commanding Officer	1
D. Rothenberger	1
Naval Undersea Warfare Center, FL	
Officer in Charge	1
R. Kennedy	1
Naval Weapons Center, CA	1
Office of the Chief of Naval Research, VA	
OCNR-00; -10; -11; -12; -13; -20; -21; -22; -23 (3)	11
P. Abraham	1
N. Gerr	1
D. Johnson	1
A. Wood	1
Space and Naval Warfare System Command, DC	
SPAWAR-00; -04; -005; PD-80; PMW-181	5
R. Cockerill	1
L. Parrish	1
U. S. Air Force, Maxwell Air Force Base, AL	
Air University Library	1
U. S. Department of Commerce, CO	
A. Spaulding	1
Vandenberg Air Force Base, CA	
R. Leonard	1

INITIAL DISTRIBUTION LIST (CONT'D)

Addressee	Number of Copies
Brown University, RI	
Documents Library	1
Drexel University, PA	
S. Kesler	1
Duke University, NC	
J. Krolik	1
Harvard University, MA	
Gordon McKay Library	1
Johns Hopkins Applied Physics Laboratory, MD	
J. Costabile	1
Johns Hopkins University, MD	1
Kansas State University, KS	
B. Harms	1
Lawrence Livermore National Laboratory, CA	
Director	1
L. Ng	1
Los Alamos National Laboratory, NM	1
Marine Biological Laboratory, MA	1
Massachusetts Institute of Technology, MA	
Barker Engineering Library	1
Northeastern University, MA	
C. Nikias	1
Pennsyvania State University, PA	
Director	1
R. Hettche	1
E. Liszka	1
F. Symons	1
Rutgers University, NJ	
S. Orfanidis	1
San Diego State University, CA	
F. Harris	1
Sandia National Laboratory, NM	
Director	1
J. Claasen	1
Scripps Institution of Oceonography, CA	1
Southeastern Massachusetts University, MA	
C. Chen	1
Syracuse University, NY	
D. Weiner	1
United Engineering Center, NY	
Engineering Societies Library	1
University of Colorado, CO	
L. Scharf	1
University of Connecticut, CT	
Wilbur Cross Library	1
C. Knapp	1

INITIAL DISTRIBUTION LIST (CONT'D)

Addressee	Number of Copies
University of Florida, FL	
D. Childers	1
University of Illinois, IL	
D. Jones	1
University of Michigan, MI	
Communications and Signal Processing Laboratory	1
W. Williams	1
University of Minnesota, MN	
M. Kaveh	1
University of Rhode Island, RI	
Library	1
G. Boudreaux-Bartels	1
S. Kay	1
D. Tufts	1
University of Rochester, NY	
E. Titlebaum	1
University of Southern California, CA	
W. Lindsey	1
A. Polydoros	1
University of Texas, TX	1
University of Washington, WA	
Applied Physics Laboratory	1
D. Lytle	1
J. Ritcey	1
R. Spindel	1
Villanova University, PA	
M. Amin	1
Woods Hole Oceanographic Institution, MA	1
Yale University, CT	
Kline Science Library	1
A. Nehorai	1
P. Schultheiss	1

INITIAL DISTRIBUTION LIST (CONT'D)

Addressee	Number of Copies
Accurate Automation, TN	
P. Simpson	1
Advanced Acoustic Concepts, MD	
F. Rees	1
Analysis and Technology, CT	
Library	1
Analysis and Technology, VA	
D. Clark	1
Bell Communications Research, NJ	
D. Sunday	1
Berkeley Research, CA	
S. McDonald	1
Bolt, Beranek, and Newman, CT	
P. Cable	1
Bolt, Beranek, and Newman, MA	
H. Gish	1
EDO Corporation, NY	
M. Blanchard	1
E G & G, VA	
D. Frohman	1
General Electric, MA	
R. Race	1
General Electric, NJ	
M. Allen	1
H. Urkowitz	1
Harris Scientific Services, NY	
B. Harris	1
Hughes Aircraft, CA	
T. Posch	1
International Business Machines, VA	
G. Demuth	1
Kildare Corporation, CT	
R. Mellen	1
Lincom Corporation, MA	
T. Schonhoff	1
Magnavox Electronics Systems, IN	
R. Kenefic	1
MSB Systems, CT	
A. Winder	1
Nichols Research, MA	
T. Marzetta	1
Northrop Corporation, CA	
R. Nielsen	1
Orincon Corporation, CA	
J. Young	1

INITIAL DISTRIBUTION LIST (CONT'D)

Addressee	Number of Copies
Orincon Corporation, VA	
H. Cox	1
Prometheus, RI	
M. Barrett	1
J. Byrnes	1
Raytheon, RI	
P. Baggenstoss	1
R. Conner	1
S. Reese	1
Rockwell International, CA	
D. Elliott	1
Schlumberger-Doll Research, CT	
R. Shenoy	1
Science Applications International Corporation, CT	
F. DiNapoli	1
Science Applications International Corporation, VA	
P. Mikhalevsky	1
Sperry Corporation, NY	1
Toyon Research, CA	
M. Van Blaricum	1
Tracor, TX	
T. Leih	1
B. Jones	1
K. Scarbrough	1
TRW, VA	
R. Prager	1
G. Maher	1
Westinghouse Electric, MA	
R. Kennedy	1
Westinghouse Electric, MD	
H. Newman	1
Westinghouse Electric, MD	
R. Park	1